UNNS Substrate Research Program | Cross-Domain Synthesis Manuscript

Nature as Structural Motion: A Cross-Domain UNNS Synthesis

Synthesized from thirteen `regime_synthesis` research branches: predictive admissibility search · boundary-mediated structural continuity · non-crossability · charge boundary routing · color confinement · cosmological boundary routing · stellar boundary dynamics · extreme physical transitions · galaxy structure and validation · UNNS-H Mode plasma confinement · time crystal · multi-clock recurrence · turbulence (JHTDB)

Status: Synthesis manuscript, corpus-scoped · Date: 2026

Abstract

Thirteen separately developed UNNS (Unbounded Nested Number Sequences) research branches have each asked, within their respective empirical scopes — domain-specific in most cases, cross-domain in a few — how a system's representation as an admissible structure changes under a physical, observational, or representational transformation. Read individually, each branch reports a branch-specific result: a cosmological bounce, a supernova light curve, a charge-conserving decay, a tokamak edge transition, a turbulence cascade, classification of a time-crystal candidate. Read together, a narrower and more specific pattern becomes visible than the earlier, looser claim that "systems move through admissibility space." Across the examined corpora, physical structure is repeatedly characterized not only by the admissible region a system occupies, but by a small, recurring vocabulary of ways structural change can be organized: trajectories can persist while deforming, approach a boundary without crossing it, turn at a finite locus, or branch into more than one downstream regime, while admissibility-relevant relations among transformations can preserve or repair a closure route, recover continuity between representational charts, recur under a temporal grammar, or approximately commute between two transformation orders. This manuscript names and formally distinguishes eight such *structural motion classes*, traces each to the specific branch corpora that support it (cosmological turning-locus routing [8], stellar catastrophic branching [9], charge- and color-closure preservation [5, 6, 7], H-mode plasma edge-route preservation [12], representation-recoverable neutrino, spectral, and supernova ladders [4, 3, 10], galaxy structural persistence and its representation sensitivity [11], temporal recurrence and its two documented grammar-domain boundaries [13, 14], and scale–time commutation in forced isotropic turbulence [15]), and assembles a cross-domain evidence matrix summarizing initial regime, transformation, motion class, boundary behavior, representation effect, and validation type for each branch. Consistent with the source program's stated practice, the synthesis is organized around three explicitly separated claim tiers — corpus-scoped observed patterns, framework-level interpretations, and open conjectures — and gives a dedicated, non-abbreviated treatment to the program's negative and boundary-encountering results, including a partial turbulence replication, two independent temporal-recurrence grammars that each encountered a domain boundary at the same quasi-periodic candidate, and a static whole-galaxy transfer test that did not clear its preregistered confirmation gate. The emerging picture is that the object of study across this corpus is not merely admissible structure, but admissible *structural motion*.

Contents

1 Introduction: From Structural States to Structural Motion

The UNNS Substrate Research Program has, across more than a dozen domain-specific branches gathered under the `regime_synthesis` archive, repeatedly asked a single question in different physical settings: does a given physical system, represented as an ordered structural sequence, remain inside the admissible region $\mathcal{M}_{\mathrm{adm}}$ of realizability space under a specified transformation? Early UNNS work answered this question state-by-state: a ladder is evaluated, a verdict is returned (FULL_PERCOLATION or HARD_FRAGMENTATION under STRUC-PERC-I; a regime and state under STRUC-I), and the verdict is reported as a property of the system at that moment.

The thirteen branches synthesized here were not designed as a single experiment. They were developed separately, by different sub-programs of the same research effort, spanning cosmology, core-collapse supernovae, tokamak plasma confinement, particle and hadron physics, molecular and atomic spectroscopy, protein folding, galactic dynamics, forced isotropic turbulence, and discrete time-crystalline recurrence. "Separately developed" is a deliberate choice of word over "independently developed": several branches were written by different sub-programs at different times but nonetheless draw on the *same* underlying corpus (the 67-ladder neutrino detector corpus and the Voyager 1 heliopause record each recur across three branches; see Section 2 for the full dependency map). Thirteen branches are not thirteen independent confirmations of a shared pattern in the statistical sense of that word; Section 2 states precisely how much independence the corpus does and does not supply before the taxonomy is used to interpret that pattern. Read individually, each branch supports a domain-scoped empirical claim. Read together, they support a claim about the recurring *kinds of change* a structural state can undergo while remaining inside, approaching, or productively re-entering $\mathcal{M}_{\mathrm{adm}}$.

Central thesis. *Across the examined* UNNS *corpora, physical structure is better characterized not only by the admissible region it occupies, but by the constrained forms of structural motion and transformation relation through which it can persist, approach a boundary, turn, branch, preserve closure, recover across charts, recur under a grammar, or participate in approximately commuting transformation orders.*

Scope of the present synthesis. *This statement does not identify structural motion with the* UNNS *Substrate as a whole. Within the wider* UNNS *architecture, structural motion begins only after questions of structural generation, representation, and admissibility have been posed. The contribution of this manuscript is to show that the transformation layer itself exhibits recurrent organization across the examined corpora.*

This is a narrower and more specific claim than an earlier, looser formulation according to which "systems move through admissibility space." The distinction matters because the collected branches do not report one undifferentiated kind of motion: a cosmological bounce, a supernova progenitor's routing into distinct post-collapse regimes, a charge-conserving particle decay, and a scale–time commutation test in turbulence are not the same kind of trajectory, even though all four are evaluated with closely related UNNS instruments (STRUC-PERC-I, STRUC-I) and vocabulary (admissibility, percolation, connectivity margin). This manuscript's task is to make that difference explicit: to distinguish *structural state* from *structural motion*, and to name the small number of motion classes the corpus actually supports.

1.1 Organization

Section 2 addresses a methodological question that must be settled before any cross-branch pattern is interpreted: which of the thirteen branches share an underlying corpus, and what that sharing does and does not license the synthesis to claim. Section 3 fixes notation and recalls, without re-deriving, the formal apparatus (admissibility manifold, Universal Structural Law, Margin-Confinement Law) that the branch manuscripts share, and introduces the manuscript's own synthesis-level notation for structural state, transformation, and trajectory. Section 4 reviews the static organization of $\mathcal{M}_{\text{adm}}$ — basins, margins, and fingerprints — as the backdrop against which motion is defined. Section 5 introduces the taxonomy of eight structural motion classes. Sections 6–10 develop each class (or cluster of classes) against its supporting branch corpora. Section 11 assembles the cross-domain evidence matrix. Section 12 collects the program's negative and boundary-encountering results. Section 13 proposes a Structural Motion Principle at the appropriate epistemic register. Section 14 lists open problems, and Section 15 concludes.

1.2 Claim tiers

Following the source program's own scope discipline, every substantive claim in this manuscript is tagged with one of three tiers, and the tag is treated as part of the claim rather than as decoration:

- [Observed] — a pattern directly reported, with specific numbers or verdicts, in one or more of the thirteen branch corpora. An observed pattern is corpus-scoped: it is not asserted to hold outside the tested domain and sample.
- [Interpretation] — a synthesis-level reading that connects observed patterns across two or more branches. An interpretation is the present manuscript's own contribution and is not separately validated by any single branch corpus.
- [Conjecture] — an explicitly open, more ambitious statement (for example, that a domain-independent taxonomy of structural motion exists) that the corpus is consistent with but does not establish.

1.3 Structural motion within the UNNS Substrate

Structural motion is not proposed here as a complete definition of the UNNS Substrate. It is one layer of a broader structural program. The Substrate first requires a representation of a system as an ordered structural object; asks whether that representation is admissible; studies the internal organization of admissible space; and only then asks how admissible structure may transform. The present manuscript addresses primarily this fourth question.

Figure 1 locates that fourth question within the larger structure. The solid chain — Representation → Admissibility → Organization → Structural Motion → Toward Selection/Prediction — is the architecture this synthesis actually establishes, with the final stage named accordingly, since it is touched on but not fully developed here: Section 3 fixes the representation $S = (L, c, \chi)$ and the admissibility criterion $\mathcal{M}_{\text{adm}}$ (Eq. (1)); Section 4 reviews the organization of admissible space into basins, margins, and fingerprints; Sections 5–11 develop structural motion itself — the eight classes that are this manuscript's central subject; and Section 10 touches, without fully developing, the question of which admissible routes a system is likely to select or occupy next. A wider UNNS program architecture — Generation → Representation → Admissibility → Organization → Transformation → Selection → Prediction — also asks how admissible structures can be *generated* in the first place, and treats route-selection and prediction as two distinct later stages rather than one. That wider chain is shown dashed and greyed in Figure 1: it is not a claim this synthesis establishes, since the present corpus does not develop the generability layer in sufficient depth to support it here, and it is shown only to locate this manuscript's contribution within the larger program, not to argue for it.

In short, the relation is one of proper inclusion, not identity: the UNNS Substrate is not the eight motion classes of Section 5, and this manuscript's central claim is not that those eight classes exhaust the Substrate, but that, within it, admissibility alone is insufficient to characterize change — the admissible *modes* of change are themselves structured.

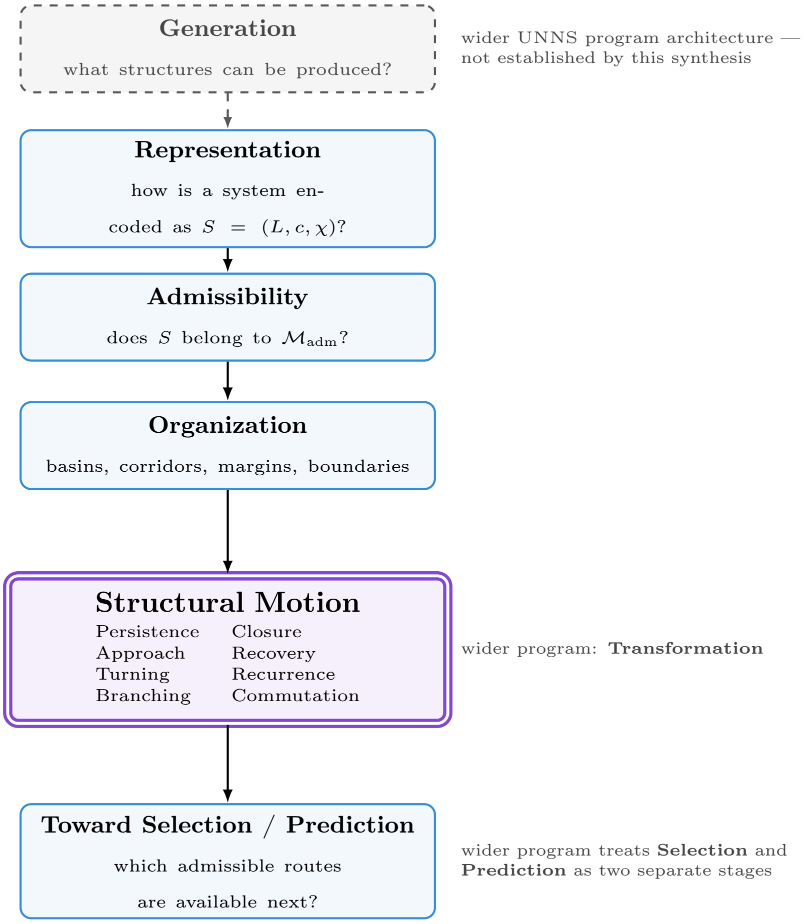

Figure 1: Structural motion within the UNNS Substrate. The solid chain is the architecture this manuscript establishes: a structural state is represented, tested for admissibility, organized into basins and margins (Section 4), and then examined for the ways it can transform — structural motion, developed in Sections 5–11 and shown here as the eight classes inside the emphasized double-bordered box. The final stage is labeled "Toward Selection / Prediction" rather than "Selection / Prediction" because Section 10 touches this question without fully developing it; it is not established here to the same degree as the preceding four stages. The dashed Generation box and the grey annotations mark the wider UNNS program's own architecture, in which a prior generability layer and a later separation of route-selection from prediction are also posed; that wider architecture is not established by the present synthesis and is shown only to locate this manuscript's contribution within it, not to assert it.

2 Synthesis Methodology and Corpus Dependency

Before any cross-branch pattern in Sections 5–11 is read as thirteen separate confirmations of a shared structural vocabulary, it is necessary to state plainly how much statistical independence the thirteen branches actually supply. They do not supply thirteen independent draws from thirteen disjoint corpora. Several branches consume, in whole or in large part, the same underlying data as other branches, and at least one branch (Canonical Structures in Admissibility Space [2]) is explicitly constructed as a cross-corpus persistence-geometry study built substantially from ladders already analyzed in earlier branches, rather than from a corpus of its own.

Governing principle. *Thirteen branches are not thirteen independent confirmations of a shared structural pattern. They are thirteen structural* analyses*, several of which examine the same physical corpus through a different instrument, transform, or question. Independence must be assessed at the level of corpora, not at the level of branch manuscripts.*

2.1 A corpus dependency map

Table 1 traces each physical corpus used anywhere in the synthesized branches to every branch that draws on it, based on matching sample sizes, instrument records, and explicit cross-citations in the underlying manuscripts (branch [3], for instance, is cited by name inside [2] as the source of its chemistry corpus and stitching-defect pattern, and both report the same 80.4% single-isolate-node figure for that corpus).

A point of terminology follows directly from this table and is worth stating explicitly, since "supernova" corpora appear in three different branches under three different physical meanings that share no data: the Type Ia raw-magnitude and Δ-magnitude ladder in Extreme transitions [10] is a standardized-candle brightness sequence; the core-collapse progenitor/light-curve/spectral-evolution corpus in Stellar boundary dynamics [9] is a structurally unrelated three-phase bridge of a different explosion mechanism; and Planck-2018-anchored ΛCDM parameters in Cosmological routing [8] use supernova-calibrated cosmological distances only as background input, not as a structural ladder in their own right. These should not be read as three views of one corpus.

2.2 What this does and does not license

Of the eight physical/observational corpora with no confirmed or likely overlap (charge PDG data, lattice-QCD confinement diagnostics, TCV/MAST plasma events, the cosmological bridge corpus, the stellar ABC corpus, the SPARC galaxy sample, the JHTDB turbulence cutouts, and the time-crystal calibration corpora), each supports at most one or two motion classes in Section 5. These eight physically and observationally distinct corpus families, collected by different sub-programs using different instruments at different times, constitute the **genuinely independent empirical core** from which the cross-domain taxonomy of Section 5 is synthesized; they are evidence for the taxonomy, not a separate confirmation of it after the fact, and later branches (below) are best read as tests of the taxonomy's recoverability and robustness rather than as additional independent discoveries of it. Six branches require an additional reuse qualification, divided into two different kinds that should not be conflated. Four branches — non-crossability [4], boundary-mediated continuity [3], predictive admissibility [2], and extreme transitions [10] — substantially reanalyze that same set of independent corpora (principally neutrino, Voyager, and Nevada) through different instruments and questions (representation recovery, margin confinement, adversarial falsification). Separately, the two temporal-recurrence branches [13, 14] share only the prospective candidate C003 while each using its own independently frozen

Corpus	**Branches sharing it**	**Status**
Neutrino detector ladders (67, two pipeline stages: raw and Δ-lifted; TMVA/DeepL encodings)	Non-crossability [4]; Boundary-mediated continuity [3]; Predictive admissibility [2]	**Confirmed shared.** Identical ladder count (67) and identical headline recovery statistic (9/9 fragmented ladders recover under Δ-lifting) recur verbatim in all three; both [4] and [3] trace to the same standalone Neutrino Detector Observational Corpus report.
Voyager 1 heliospheric transit (3,500 magnetic-field windows, 2011–2017)	Non-crossability [4]; Extreme transitions [10]; Predictive admissibility [2]	**Confirmed shared.** Identical evaluation count (3,500) and identical 97.4% Full-percolation figure recur in all three.
Nevada nuclear-explosion station-events (29 events)	Non-crossability [4]; Extreme transitions [10]; Boundary-mediated continuity [3] (cited, not independently re-evaluated)	**Confirmed shared.** [3] discusses this corpus's IC.MDJ station result as an instance of its own Universal Stitching Pattern but attributes the underlying evaluation to [10]; it is not an independent measurement.
Metallic-glass / oxide spectral chemistry (SciGlass; 500 ladders in [3], a 69-ladder normalized-oxide subset in [2])	Boundary-mediated continuity [3]; Predictive admissibility [2]	**Confirmed related, not confirmed identical.** [2] cites [3] by name as the source of the 80.4% single-isolate stitching figure it reuses; the 69-ladder oxide subset is evidently drawn from or normalized against the same source chemistry corpus, but the exact ladder-level overlap between the 500- and 69-ladder sets is not independently verifiable from the material available to this synthesis.
Protein Markov State Model (Folding@home conformational dynamics)	Boundary-mediated continuity [3] (5 ladders, unspecified protein system, 5,000 conformational states); Predictive admissibility [2] (QT45 ribozyme)	**Likely related, not confirmed identical.** Both report a Markov-state ladder with exactly three isolated/kinetically-trapped nodes interpreted as conformational traps, from a Folding@home source; the two manuscripts name the underlying molecular system differently (an unspecified protein in [3] versus a ribozyme in [2]), so this synthesis flags the match rather than asserting corpus identity.
Time-crystal candidate C003 (two-clock discrete time quasi-crystal)	Time crystal [13]; Multi-clock recurrence [14]	**Confirmed shared candidate, independently frozen grammars.** Both branches test the same physical candidate, but on separately frozen development/calibration corpora that each explicitly exclude C003 from grammar construction (Finding 9.1); this is cross-validation *by construction*, not corpus duplication, and is the one case in this table where re-use strengthens rather than weakens the independence of the resulting agreement.

Table 1: Corpora used in more than one synthesized branch. Corpora not listed here (charge-sector PDG particle data [5, 6]; lattice-QCD-derived confinement diagnostics [7]; TCV/MAST tokamak plasma events [12]; the cosmological three-route bridge corpus [8]; the core-collapse supernova ABC corpus [9]; the SPARC galaxy sample [11]; the JHTDB turbulence cutouts [15]; and the time-crystal calibration/development corpora proper, as opposed to the shared candidate C003) are, on the evidence available to this synthesis, used in exactly one branch each.

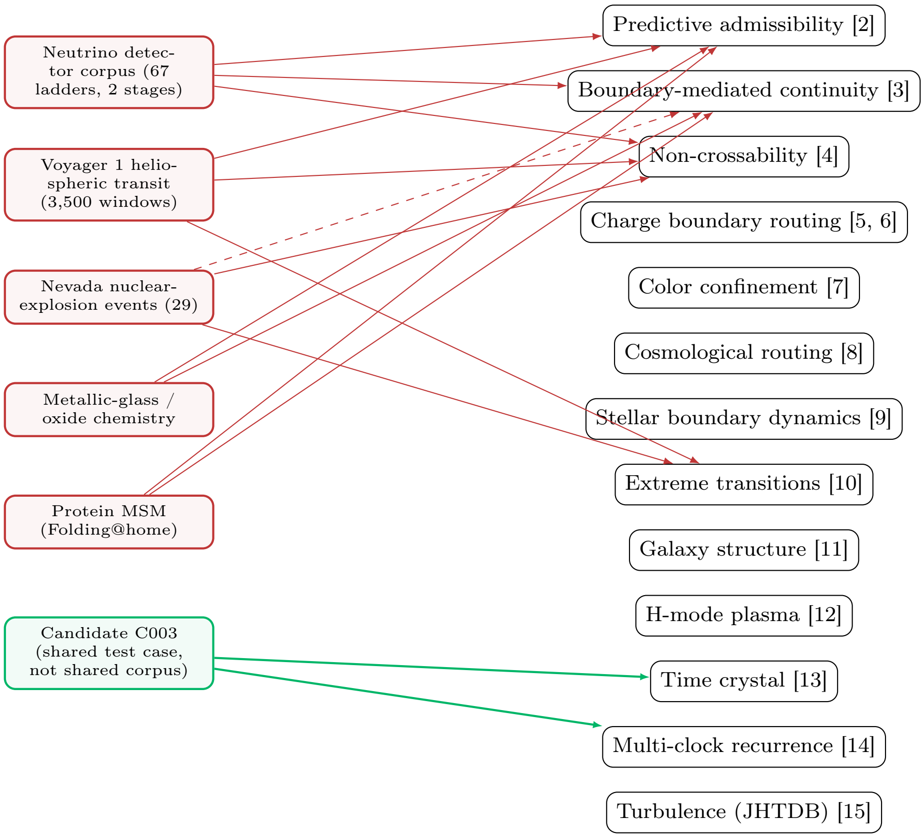

Figure 2: Evidence dependency map. Left: physical corpora used in more than one branch (Table 1). Right: all thirteen branches. An orange/red arrow marks corpus reuse (the target branch re-analyzes, rather than independently collects, that corpus; a dashed arrow marks a cited-but-not-independently-re-evaluated case); a green arrow marks the one case of a shared *candidate* tested against independently frozen grammars, which strengthens rather than weakens the resulting agreement (Section 9.1). Branches with no incoming orange/red arrow — charge routing, color confinement, cosmological routing, stellar boundary dynamics, galaxy structure, H-mode plasma, turbulence, and both time-crystal branches (whose only incoming arrows are the green shared-candidate relation, not corpus reuse), nine of thirteen — draw on no corpus shared with another branch in this corpus, on the evidence available to this synthesis; these, together with each time-crystal branch's own independently frozen calibration corpus, are the genuinely independent core referred to in Section 2.2.

development/calibration corpus (Figure 2); this is cross-validation of a shared test case under two independently constructed grammars, not ordinary corpus reuse, and it is not counted among the overlaps above. The first kind of reuse is scientifically valuable — it is exactly how a recovery mechanism like Δ-lifting gets tested against genuinely different questions rather than validated once and assumed — but it means the correct description of the corpus is *eight non-overlapping empirical corpus families, several of them re-examined by up to three distinct structural instruments each*, not thirteen independent confirmations. Table 3 and the motion-class attributions of Section 5 onward should be read with this qualification attached; it is not repeated at every subsequent mention.

This dependency structure also explains, rather than merely excuses, an accounting question a careful reader will notice in Section 3: the six evaluation categories cited there from [4] (5,233 + 9,826 + 81 + 29 + 3,500 + 67) are an abridged excerpt of a fuller table in the source manuscript that also separately reports Voyager 2 kinematic and density channels, the SN Ia and Nevada-seismic sub-splits, and a second (post-Δ-lift) neutrino pass; even the fuller breakdown, reconstructed from the source manuscript's own Table 5, does not sum cleanly to the source's own stated aggregate of $N_{\text{tot}} = 15{,}401$ evaluations. This synthesis has not been able to resolve that residual discrepancy from the material available to it, and states it here as an open accounting question in the source corpus rather than silently adopting either figure as authoritative.

3 Formal Setting

3.1 Admissibility and the Universal Structural Law

The shared substrate beneath all thirteen branches is the admissibility inequality established in the program's foundation document [1]: for a ladder L (an ordered physical sequence $L_1 \leq L_2 \leq \cdots \leq L_n$) and a perturbation scale ε,

$$\operatorname{inv}(P_\varepsilon;\, L) \;\leq\; \nu(V_\varepsilon(L))\,, \tag{1}$$

where P_ε is a family of perturbation operators, $\operatorname{inv}(\cdot)$ is the perturbation-invariant fraction of L, and $\nu(V_\varepsilon(L))$ is the admissibility volume of its ε-neighborhood. Foundations of the UNNS Substrate reports zero hard violations of Eq. (1) at physical parameter values across a multi-domain corpus exceeding 1,500 ladders and 150,000 assessments, and formalizes this empirical regularity as the **Universal Structural Law (USL)**: the admissibility inequality is the measurable projection of an invariant structural condition on relational configurations, not merely a descriptive regularity [1]. The admissibility manifold is defined equivalently as an operator pre-image, $\mathcal{M}_{\text{adm}} := \Sigma^{-1}(1)$ for a selection operator Σ, and geometrically as $\mathcal{M}_{\text{adm}} = \{(L, c) \in \mathcal{L} \times C : A_\kappa(L, c) \leq 1\ \forall \kappa \in \mathcal{K}\}$, closed in the product topology [1].

This construction should be located relative to an established literature this synthesis does not claim to supersede. The idea that a system occupies a region of admissible or stable configurations, bounded by a qualitatively distinguished set of transitions, is the organizing idea of structural-stability and bifurcation theory: Andronov and Pontryagin's original "coarse systems" [20], Peixoto's structural-stability theorem on two-dimensional manifolds [21], and the standard modern treatments of bifurcation and attractor geometry [16, 17, 18, 19, 26]. $\mathcal{M}_{\text{adm}}$ and a basin of attraction are not asserted to be the same mathematical object — $\mathcal{M}_{\text{adm}}$ is defined by the admissibility inequality on a ladder representation, not by a flow's asymptotic behavior — but the kinship is close enough that the boundary and basin vocabulary of Sections 4–5 should be read as continuous with, not independent of, this tradition. Catastrophe theory's treatment of qualitative transitions between stable configurations [22, 23] and the critical-transitions literature that treats an approaching bifurcation as empirically anticipatable from a system's own dynamics [24, 25] are the closest external analogues to, respectively, the branching and turning motion classes of Section 5 and the boundary-approach diagnostics of Section 6.1; the parallel is suggestive rather than demonstrated to be exact; none of these external results is used to derive any UNNS claim, and Section 2's corpus-dependency discipline applies to internal branches only, not to this external context.

3.2 The Margin-Confinement Law

The branch most directly relevant to structural *motion* is the Margin-Confinement Law [4], which proves — for flows satisfying an explicit identity-preserving condition (Definition 3 of [4], conditions IPF-1 through IPF-4) — that a trajectory beginning in $\mathcal{M}_{\text{adm}}$ cannot cross $\partial\mathcal{M}_{\text{adm}}$ into the Hard regime:

Theorem 3.1 (Margin-Confinement Law, after [4])**.** *Let* $L_0 \in \mathcal{M}_{\text{adm}}$ *and let* $\{L_t = \Phi_t(L_0)\}_{t\geq 0}$ *be an identity-preserving flow in the sense of the source manuscript's Definition 3. Then* $\Phi_t(L_0) \in \mathcal{M}_{\text{adm}}$ *for all* $t \geq 0$*. Persistent Hard outcomes under such a flow are projection or representation artifacts, not genuine dynamical transitions.*

The qualifier is load-bearing: Theorem 3.1 constrains *identity-preserving flows* specifically, and the source manuscript is explicit that discontinuous identity rupture, non-admissible initial conditions, degenerate or under-sampled projections, and externally imposed fragmentation lie outside its scope [4]. Within that scope, the law also supplies the sharpest available statement of the approach/crossing distinction that motion class 5.2 below is built on:

Proposition 3.2 (Asymptotic Boundary Accessibility, after [4])**.** $m(L_t) \to 0^+$ does not imply $L_t \notin \mathcal{M}_{\text{adm}}$. Admissibility persists under arbitrarily small positive connectivity margin; $\partial\mathcal{M}_{\text{adm}}$ is asymptotically accessible but never realized in finite time under identity-preserving flow.

Across its corpus of 5,233 admissibility evaluations, 9,826 phase-mapping evaluations, 81 cross-domain percolation evaluations, 29 nuclear station-events, 3,500 Voyager 1 heliopause windows, and 67 neutrino detector ladders, [4] reports no genuine crossing (at 99% confidence, an upper bound on the genuine-crossing rate of $p < 3.0 \times 10^{-4}$) and formalizes the mechanism by which apparent crossings arise despite this: **Representation-Induced Structural Collapse (RISC)**, an observed Hard verdict produced by a representation or projection that itself breaks an IPF condition, rather than by a genuine loss of admissibility [4]. RISC and its principal repair operator, **Δ-lifting** (the local-gap transform $\Delta L = (|x_2 - x_1|, |x_3 - x_2|, \ldots)$), recur throughout Sections 7–8 below as the technical machinery underlying recoverable motion.

3.3 A unifying notation: state, transformation, trajectory

The thirteen branches use closely related but not identical formal vocabularies: $\mathcal{M}_{\text{adm}} = \{(L, c)\}$ from the foundation document [1]; a route tuple $(Q, \ell, r, \mathcal{C}, b, s_{\text{comp}})$ in charge boundary routing [6]; a phase-sign vector $\bar{\Sigma}_P$ in cosmological routing [8]; a multichannel fingerprint $F_g(\kappa) = \{\rho_g(\kappa), D_{A,g}(\kappa), \tilde{\nu}_g(\kappa)\}$ in galaxy structure [11]. Each is correct and sufficient within its own branch. None is shared across branches, which is precisely why Section 5 below needs its own notation: not a replacement for any branch's formalism, but a synthesis-level scaffold, introduced here for the first time and used only at the interpretation tier, that lets a single vocabulary describe what varies (a state), what changes it (a transformation), and what a path of changes looks like (a trajectory), across all thirteen.

Definition 3.3 (Structural state). A **structural state** is a triple $S = (L, c, \chi)$, where:

- L is the **ladder**: an ordered physical sequence $L_1 \leq L_2 \leq \cdots \leq L_n$, in the sense already fixed by the foundation document [1]. L is the object whose admissibility Eq. (1) evaluates.
- $c \in C$ is the **chart**: the representational, observational, or instrumental encoding under which L is expressed — raw versus Δ-lifted, magnitude versus orientation-signed, TMVA versus deep-embedded, coarse versus refined. (L, c) together is exactly the admissibility-manifold point of [1]: $\mathcal{M}_{\mathrm{adm}} = \{(L, c) : A_\kappa(L, c) \leq 1 \ \forall \kappa\}$.
- χ is an **auxiliary route/closure coordinate**: whatever additional structural information, beyond the scalar admissibility verdict on (L, c), is required to determine whether the state participates in a closure, an orientation, or a downstream regime assignment. χ is branch-specific in content — a closure label in charge routing, an orientation sign in cosmological routing, a downstream-regime tag in stellar branching — and is formally trivial ($\chi = \varnothing$) in branches where no such structure is needed (for example, plain persistence or grid-invariance testing).

$S = (L, c, \chi)$ is a synthesis-level construction: no single branch manuscript uses this exact triple, and it is not claimed to replace any branch's own formalism. It exists to let the eight motion classes below be stated as properties of one kind of object.

Definition 3.4 (Transformation and trajectory). A **transformation** is a map $T : S_i \to S_j$ between two structural states. A **trajectory** $\Gamma_T = \{S(t)\}_{t \in \mathcal{T}}$ is an ordered sequence of states connected by one or more transformations, indexed by a parameter t that may be physical time, a deformation-sweep index, a κ-grid configuration index, or a recurrence depth, depending on the branch. A motion class (Section 5) is a predicate on Γ_T, not on any single $S(t)$: it asks how L, c, or χ change, together or separately, along the trajectory, not what any one state's verdict is.

This notation makes explicit a distinction implicit throughout the branch corpus and load-bearing for the taxonomy: a transformation can act on L alone (a genuine physical evolution: the ladder's underlying values change), on c alone (a change of chart with L physically unchanged: Δ-lifting, re-encoding, re-embedding), or on χ alone (a change of route/closure bookkeeping with neither the physical ladder nor its numerical chart changing: for instance, reclassifying which downstream regime a branching event routes to, without altering any measured value). Conflating these is exactly the error Interpretation 8.1 warns against; Section 3.4 makes the distinction load-bearing by using it as a second, independent classification axis.

3.4 Four kinds of transformation

The eight motion classes of Section 5 classify *trajectories*. A second, independent axis classifies the *transformations* that produce them, and is necessary to avoid a specific conflation risk: naming a cosmological bounce and a representational Δ-lift both "turning" or both "recoverable motion" would treat a change to L as equivalent to a change to c, even where both happen to instantiate the same motion class. This synthesis distinguishes four transformation types, applied consistently across Sections 6–10:

$$\text{physical evolution} \neq \text{chart transformation} \neq \text{analytical operator} \neq \text{temporal evolution.}$$

- **Physical evolution (P).** T acts on L: the underlying physical system genuinely evolves, in a sense every branch would recognize as a dynamical change, independent of how it is observed or encoded. Example: the cosmological contraction–bounce–expansion sequence, or core-collapse supernova routing.
- **Chart transformation (R).** T acts on c with L held fixed: the same physical system is re-expressed in a different observational or numerical chart. Example: Δ-lifting; magnitude-only versus orientation-signed cosmological encoding; raw versus normalized chemistry ladders.
- **Analytical operator (O).** T acts on the instrument, analysis pipeline, or admission criterion applied to a fixed (L, c): a different κ-grid configuration, a different embedding or classifier, a different admission-gate construction, a different deformation-field sweep imposed by the analysis rather than observed as a physical change. Example: the seven-configuration grid-invariance sweep [3]; TMVA versus deep-learning embedding of the same raw neutrino ladders [3]; the 9×9 deformation-field sweep in fundamental-constant space [2]; the frozen recurrence-admission gate and the integer-depth versus multi-clock grammars applied to the same candidate [13, 14].
- **Temporal evolution (T).** T is the physical system's own sequential or recurring structure along an ordering parameter, considered prior to and independent of whatever analytical grammar is later used to test it. Example: the time-ordered recurrence-depth sequence $C(q)$ traced along candidates C001/C002 [13], before any admission gate is applied to it.

A related clarification is needed for embedding and other representation-producing analyses. Definition 3.3 lists TMVA versus deep-embedded encodings as examples of the chart c, while the classification above lists the choice between TMVA and deep-learning embedding as an instance of the analytical operator (O); this is not a conflict once the two statements are read as describing different parts of the same transformation. The *embedding algorithm* — the choice to apply TMVA, deep-learning embedding, or another encoding procedure to a fixed (L, c) — is classified as the operator O_{embed}; the *encoding it produces* is the resulting chart c'. A transformation of this kind is therefore reported as $(L, c) \xrightarrow{O_{\text{embed}}} (L, c')$: an operator-classified transformation whose effect is a chart change. Deep-embedding recovery of fragmented neutrino ladders [3] (Table 2, Analytical-operator column) is accordingly best read as *operator-mediated* recoverable motion between charts, not as evidence that the operator/chart distinction collapses.

A recurrence test therefore typically requires *both* T and O, and this is a feature of the classification rather than a gap in it: T supplies the temporal trajectory being examined, and O supplies the grammar (the admission gate, or a choice between competing grammars) that tests whether that trajectory recurs. The two are kept formally distinct because a grammar can be revised, re-frozen, or replaced by a competing one without the underlying temporal trajectory changing at all, which is exactly what happens when candidate C003 is evaluated under two separately constructed grammars in Section 9.1.

Table 2 crosses the eight motion classes against these four transformation types, populating each cell only where the corpus supplies a concrete instance and marking the remainder as open rather than inferring an example that was not tested. The resulting sparsity pattern is itself informative: it shows, for example, that turning and branching have so far been tested only under physical and (for turning) chart transformations, with no analytical-operator or temporal instance yet reported for either, and that persistence has not yet been tested under a temporal transformation at all.

The Commutation row is left structurally distinct on purpose. Section 9.2 defines commutation as agreement between two transformation *orders* (scale-then-time versus time-then-scale), not as a property of a single trajectory produced by one transformation. Scale-coarsening is itself an operator-analytical transformation and time-advancement is itself a temporal one; commutation asks whether composing them one way agrees with composing them the other way. It is therefore not a ninth cell that happens to be hard to fill — it is a second-order question about two cells of this table (operator-analytical and temporal) simultaneously, and Section 5 returns to this point when it takes up whether commutation belongs to the same taxonomic level as the other seven classes.

4 Static Organization of Admissibility Space

Structural motion presupposes a structured space to move through, and three branches establish that $\mathcal{M}_{\text{adm}}$ is not occupied uniformly.

4.1 Basins and internal topology

Admissible Cluster Geometry [3] shows, across 827 ladders combined from metallic-glass spectral chemistry, liquid-scintillator neutrino detection, and protein Markov-state models, that $\mathcal{M}_{\text{adm}}$ organizes into coherent **admissible basins** connected by sparse **continuity corridors** and separated by **fragmentation barriers**, rather than forming one homogeneous admissible region [3]. Within the 500-ladder metallic-glass corpus, 368 ladders return HARD_FRAGMENTATION, but 296 of those (80.4%) fail by exactly one isolated node with mean giant ratio GR = 0.936 — what [3] terms a **stitching defect**: a graceful, localized failure that leaves the ladder geometrically inside a larger admissible cluster rather than catastrophically disintegrated. A grid-invariance test across seven κ-grid configurations (1,316 evaluations on a 188-material normalized spectral corpus) finds zero regime flips, supporting the existence of stable κ_{conn} fixed points that organize $\mathcal{M}_{\text{adm}}$ into discrete strata [3].

This vocabulary — basins, corridors, barriers, a giant-component ratio GR — is drawn directly from percolation theory [27, 28, 29], and STRUC-PERC-I is, at the implementation level, a percolation instrument. A caveat is appropriate before the parallel is used any further: classical percolation concerns path-existence on a lattice or graph under random edge/site occupation, not a scalar admissibility criterion evaluated on a continuous manifold, so the correspondence between $\mathcal{M}_{\text{adm}}$'s basin structure and a percolation cluster is structural and expository rather than a proven mathematical equivalence. Topological data analysis — persistent homology in particular [30, 31, 32] — is the more literal external analogue to what Admissible Cluster Geometry's basin topology is doing, though no branch in this corpus computes persistent homology directly; where a future UNNS branch does compute it, that literature, not the percolation analogy, is the correct point of contact. The coherent-versus-turbulent basin distinction of Section 4 (discrete strata separated by fragmentation barriers) also echoes the general phase-transition picture of a system organizing into qualitatively distinct macroscopic regimes separated by a critical boundary [33, 34], again offered as a located parallel rather than a claimed identity.

4.2 Persistence geometry and basin co-occupancy

Canonical Structures in Admissibility Space [2] reframes the question from static encoding quality to **persistence under deformation**: structural coherence is measured as survival of admissibility across a deformation field in fundamental-constant space (a 9×9 grid in $\alpha/\alpha_0, \mu/\mu_0$), over $>$ 14,000 evaluations spanning $>$ 14 physical domains, including helium spectroscopy, 69 oxide ladders, the 67-ladder neutrino corpus, Planck CMB TT/TE/EE spectra, protein conformational dynamics, and 3,500 Voyager 1 heliospheric windows. Zero hard violations occur anywhere in this corpus [2]. Physically unrelated systems are found to co-occupy the same admissibility basins at high cosine similarity on a five-dimensional admissibility vector (helium–cosmology 0.993; helium–neutrino 0.901; neutrino–cosmology 0.882), which [2] interprets structurally rather than physically:

Framework Interpretation 4.1. Co-occupancy of an admissibility basin is not identity of physical law. Physically unrelated systems occupy the same basin because the geometry of $\mathcal{M}_{\mathrm{adm}}$ constrains realizability universally; the basin geometry is the explanation, not a shared microscopic mechanism [2].

4.3 Fingerprints as a multiscale structural identity

Galaxy Structural Fingerprints [11] draws on the SPARC rotation-curve database [55] and the empirical radial acceleration relation [56] established from it, and shows that a 121-galaxy SPARC sample, represented as a multichannel structural-response fingerprint $F_g(\kappa) = \{\rho_g(\kappa), D_{A,g}(\kappa), \tilde{\nu}_g(\kappa)\}$ across a logarithmic perturbation-scale sweep, achieves near-perfect unchanged-preparation retrieval (top-1 and top-5 source recovery both 1.000; median intraclass correlation 0.99985) and organizes into a statistically preferred five-family consensus admissibility structure within a 110-galaxy Stable Structure basin (silhouette 0.825 at $k = 5$, versus 0.778–0.789 at neighboring k), separated from a discrete 11-galaxy Weak Persistence regime [11]. This is the clearest demonstration in the corpus that **persistence** — a system deforming under a perturbation sweep while remaining identifiable as itself and inside the same admissible region — is empirically well-defined and measurable at galactic scale.

5 A Taxonomy of Structural Motion

Against this static backdrop, the thirteen branches support eight structurally distinct classes of motion. Using the notation of Section 3.3, a structural state $S = (L, c, \chi)$ and a trajectory $\Gamma_T = \{S(t)\}$ organize this section around the same distinction stated in Section 1:

$$\text{structural state} \neq \text{structural motion.}$$

A state is a point (or a verdict at a point); a motion class is a predicate on Γ_T. This section gives each of the eight classes an operational definition, distinguishes it from its nearest neighbors, states which classes can and cannot co-occur on the same trajectory, and gives one canonical corpus example.

5.1 Two tiers, not eight siblings

The eight classes are not eight parallel alternatives to a single classification question. Four of them (persistence, approach, turning, branching) answer the question *what shape does* Γ_T *have in* (L, c)*-space*, holding the chart and the route/closure coordinate fixed: does the trajectory stay away from $\partial\mathcal{M}_{\text{adm}}$, move toward it, reach it and reverse, or reach it and split. Call these the **Tier-1, trajectory-shape classes**. The other four (closure preservation, recoverable motion, recurrence, commutation) do not describe the shape of a single trajectory in a single chart at all; each is a statement about a *relation*: which coordinate of S is doing the work of preserving admissibility (closure preservation), how a trajectory's verdict changes between two charts (recoverable motion), how a trajectory relates to an external temporal grammar (recurrence), or how two transformation orders relate to each other (commutation). Call these the **Tier-2, relational classes**.

Working rule. *A Tier-1 tag answers "what does this trajectory look like." A Tier-2 tag answers "why does it look that way, or how does it relate to another chart, grammar, or ordering." The two tiers are not mutually exclusive alternatives and a single branch routinely receives one tag from each tier (Table 3's "Ap, Rc" and "Pe, Rc" entries are exactly this: a Tier-1 shape tag paired with a Tier-2 relational tag, not two competing classifications of the same fact).*

This resolves, rather than sidesteps, three specific questions this taxonomy invites. First: is closure preservation a motion class in the same sense as turning, or a constraint on another motion? Under the two-tier reading it is neither exactly — it is a Tier-2 attribution (admissibility is being carried by χ, not by (L, c) alone) that can accompany a Tier-1 persistence or approach trajectory rather than compete with it. Second: is recurrence "the same level" of object as branching? No: branching is a Tier-1 statement about where a single trajectory goes; recurrence is a Tier-2 statement about whether a trajectory matches an externally supplied temporal grammar. Third: is commutation a trajectory class at all? Section 3.4 already answers this directly — commutation is a second-order relation between two transformation orders, not a predicate on one trajectory, and this is precisely why it is the clearest Tier-2 case: it has no Tier-1 analogue and cannot be assigned one.

5.2 Tier 1: trajectory-shape classes

Motion Class 5.1 (Persistence)**.** Γ_T deforms in L or c while remaining inside the same admissible structural region, with no boundary encounter. Evidenced by galaxy structural fingerprints under unchanged preparation [11], deformation-field persistence in helium and CMB spectra [2], and grid-invariant κ_{conn} strata in Admissible Cluster Geometry [3].

Distinguishing criterion. Persistence is the default, "nothing structurally eventful happens" class: $m(L_t)$ stays comfortably positive and no orientation, branching, or repair coordinate is ever invoked. It is distinguished from approach purely by boundary distance, not by any qualitative difference in mechanism; the two classes sit on the same margin axis and a corpus that samples further along a trajectory can in principle observe an initially persistent segment become an approaching one. *Canonical example:* galaxy structural fingerprint retrieval under unchanged preparation, top-1 and top-5 recovery both 1.000 [11] — persistence with no representational or physical transformation at all, the cleanest possible case.

Motion Class 5.2 (Boundary approach)**.** Γ_T moves toward reduced connectivity margin, $m(L_t) \to 0^+$, without necessarily crossing $\partial\mathcal{M}_{\text{adm}}$. Approach is not crossing (Proposition 3.2).

Evidenced by Forced Coherent Collapse across heliospheric, seismic, and nuclear-explosion corpora [4, 10].

Distinguishing criterion. Approach is a statement purely about the scalar margin m, a function of (L, c) alone; it requires no orientation coordinate χ and makes no claim about what happens after the margin minimum. This is the formal basis for separating approach from turning, addressed below. *Canonical example:* the Voyager 1 heliopause transit, κ_{conn} reaching a minimum exactly at the 2012 crossing [10, 4].

Motion Class 5.3 (Turning)**.** Γ_T reaches a finite critical locus t^* at which an explicitly defined orientation coordinate $\chi = s(t) \in [-1, +1]$ reverses sign of ds/dt, with L varying continuously across t^* (no re-initialization, no chart change) and the state remaining admissible throughout. Evidenced by the effective-LQC bounce route in cosmological boundary routing [8].

Distinguishing criterion — turning versus approach-then-recession. This is the sharpest test case in the taxonomy, because Voyager's margin also dips and later recovers (Section 6.1), and a careless reading could call that "turning" too. It is not, on the criterion just stated: turning requires a defined route/orientation coordinate χ whose reversal is demonstrated (in cosmological routing, the post-turning phase-sign vector is shown to be approximately the negative of the pre-turning vector [8]); approach-then-recovery is a claim about the scalar margin m only, with no orientation coordinate defined, still less reversed — the Voyager corpus supplies no χ and therefore cannot support a turning verdict, no matter how closely its margin curve resembles one. Turning is a χ-level (route/orientation) phenomenon; approach and its recovery are (L, c)-level (margin) phenomena. This is also why turning is currently attested in exactly one branch: it is the only branch that constructs an orientation coordinate at all, and the absence of turning verdicts elsewhere in the corpus reflects that instrumentation gap, not evidence against turning as a general phenomenon. *Canonical example:* cosmological routing Dataset B, contraction $(s : -1 \to 0)$ through a finite turning locus $(a_{\min} = 2.468 \times 10^{-32})$ to expansion $(s : 0 \to +1)$ [8].

Motion Class 5.4 (Branching)**.** One pre-boundary regime routes into more than one downstream admissible regime without either downstream regime becoming inadmissible. Evidenced by core-collapse supernova routing [9].

Distinguishing criterion. Branching and turning are the corpus's two attested resolutions of a boundary encounter: turning is a single trajectory reversing and returning along (approximately) the same route; branching is a single pre-boundary regime routing into *more than one* structurally distinct downstream regime. The two are not merely different outcomes of the same test — turning requires and reports an orientation coordinate χ, while the stellar branch instead reports downstream-regime separations ($d_{AB} = 0.401 \ll d_{BC} = 1.287,\ d_{AC} = 1.365$) with no orientation coordinate defined at all, so branching cannot currently be read as "turning into more than one direction": the corpus does not (yet) supply the shared coordinate that would make that comparison meaningful (Open Problem O5). *Canonical example:* the A_to_B_contact_with_C_branching classification of the core-collapse ABC bridge [9].

5.3 Tier 2: relational classes

Motion Class 5.5 (Closure preservation)**.** A trajectory remains admissible because a transformation preserves (or, after local tension, repairs) the route/closure coordinate χ, in a case where the scalar projection (L, c) alone does not determine admissibility. Evidenced by charge boundary routing [5, 6], color confinement [7], and H-mode plasma edge-route preservation [12].

Distinguishing criterion. Closure preservation names which coordinate of S is carrying the admissibility-relevant information; it does not, by itself, say whether the underlying trajectory is Tier-1 persistent, approaching, or branching. In the charge corpus, for example, route-transition admissibility collapses (0.985→0.859) while connectivity persists (42/42 FULL_PERCOLATION), which is naturally read as a Tier-1 persistence trajectory (the corpus stays globally connected) whose robustness is explained by a Tier-2 closure attribution (route-transition coherence, not the scalar charge value, is doing the work). *Canonical example:* the Phase 3C route-transition contrast in charge boundary routing [6].

Motion Class 5.6 (Recoverable motion)**.** An apparent structural failure under chart c becomes admissible, or a stitching defect is repaired, under a locality-preserving transform to chart c', with L unchanged. Evidenced by Δ-lifted neutrino recovery [4, 3], extreme-transition Δ-magnitude recovery [10], and deep-embedding recovery of raw-fragmented detector ladders [3].

Distinguishing criterion. Recoverable motion is a relation between two evaluations of the *same* L under two charts c and c'; it is not a claim about L changing at all, which is what separates it from every Tier-1 class and from the physical sense of "recovery" also used informally of Voyager's post-crossing κ_{conn} rebound. That rebound is a change in L over time under one fixed chart — a physical-evolution event already attributed to boundary approach and persistence in Table 2 — and it does not satisfy the chart-mediated definition of recoverable motion above, even though both are loosely called "recovery." No physical-evolution instance of this formal class has been identified in the corpus, which is why the corresponding cell of Table 2 is marked as an open combination rather than populated with the Voyager rebound. *Canonical example:* Δ-lifted recovery of 9/9 fragmented neutrino ladders, GR = 1.000 in every recovered case [4, 3].

Motion Class 5.7 (Recurrence)**.** Γ_T returns structurally under a temporal grammar — an externally supplied admission criterion on a recurrence-depth or multi-clock coordinate — rather than traveling monotonically toward or away from a boundary. Evidenced by the integer-depth time-crystal grammar and its multi-clock successor [13, 14].

Distinguishing criterion. Recurrence is a relation between a trajectory and a grammar, not a property of the trajectory read off in isolation; the same candidate (C003) can and does fail one grammar while scoring strongly on individual coordinates of a second, independently constructed grammar (Section 9.1), which would be incoherent for a Tier-1 class but is expected for a Tier-2 one — a relation can hold under one externally supplied structure and fail under another without contradiction. *Canonical example:* candidates C001 and C002 admitted under the frozen gate $C(q_0) \geq 0.15,\ F \geq 0.10,\ p \leq 0.10$ [13].

Motion Class 5.8 (Commutation)**.** Two admissible transformation orders (here, scale-then-time versus time-then-scale) applied to the same structural object agree approximately, with any disagreement itself spatially localized. Evidenced by scale–time commutation in forced isotropic turbulence [15].

Distinguishing criterion. Of the four Tier-2 classes, commutation is the only one with no possible Tier-1 reading at all: it is defined on a pair of transformations, not on a trajectory, and Section 3.4 shows it spans two transformation types (operator-analytical and temporal) simultaneously rather than occupying one cell of that table. *Canonical example:* the principal commutation-survival criterion at $z = 36.0$, $p = 0.0099$, replicated in an independent Pilot B sample [15].

5.4 Composition and exclusion rules

Within Tier 1, the four classes are, by construction, close to mutually exclusive *for a given trajectory segment*: a segment cannot simultaneously be read as staying away from the boundary (persistence) and heading toward it (approach) under the same margin trend, and turning and branching are defined as alternative resolutions of the same boundary encounter. They are not, however, mutually exclusive across an entire branch corpus, which may contain multiple segments: cosmological routing's Route B is Tier-1 approach (contraction, $s : -1 \to 0$) immediately followed by turning at the locus, reported under the single label "turning" because the source manuscript treats the full arc as one event, not because approach and turning cannot logically co-occur in sequence.

Between Tier 1 and Tier 2, co-occurrence is the expected pattern, not an edge case: a Tier-2 tag explains or qualifies a Tier-1 shape rather than competing with it. Table 3 records this directly for two branches (Boundary-mediated continuity: persistence *and* recoverable motion; Non-crossability and Extreme transitions: approach *and* recoverable motion). Several other rows record only a Tier-2 tag (closure preservation for charge, color, and H-mode; recurrence for both time-crystal branches; commutation for turbulence) with no accompanying Tier-1 tag; this reflects the scope of each branch's original question — closure, recurrence, and commutation were each branch's primary object of study, and the underlying Tier-1 shape (in every one of these cases, consistent with persistence: none of these branches reports a boundary-approaching trajectory) was not separately instrumented or reported — rather than evidence that Tier-1 and Tier-2 are alternatives. This synthesis records that observation here without retroactively amending Table 3 with Tier-1 tags the source branches did not themselves report.

The one firm exclusion rule this corpus supports is definitional rather than empirical: turning (Tier 1) requires a demonstrated reversal of an explicit orientation coordinate χ, so no branch lacking such a coordinate can be assigned a turning tag regardless of how its margin curve behaves (Section 5.2). Every other pairing among the eight classes is, on present evidence, either attested or simply untested (Table 2's blank cells) rather than formally excluded.

Sections 6–10 develop these eight classes against their supporting corpora, in four clusters: boundary motion (approach, turning, branching); route preservation and closure; recoverable motion under representation change; and recurrence/commutation as transformation-algebra questions.

6 Boundary Motion: Approach, Turning, and Branching

6.1 Approach without crossing

Beyond Fragmentation [10] supplies the empirical precursor to the Margin-Confinement Law's theoretical mechanism [4]: a **Margin Collapse Hypothesis** under which explosive, impulsive, or forced transitions are characterized by systematic contraction of the local connectivity margin, $m(L_t) \to 0^+$, formalized as **Forced Coherent Collapse (FCC)**: tail dominance $\mathrm{TD} > 0.80$ together with giant ratio $\mathrm{GR} \geq 0.97$ across the κ-sweep. The clearest case is the Voyager 1 heliopause transit: across 3,500 magnetic-field windows (2011–2017), 97.4% return FULL_PERCOLATION; κ_{conn} reaches a minimum exactly at the 2012 heliopause crossing and recovers by a factor of 1.6–2.4× afterward, with the single Hard window an isolated 2011 anomaly

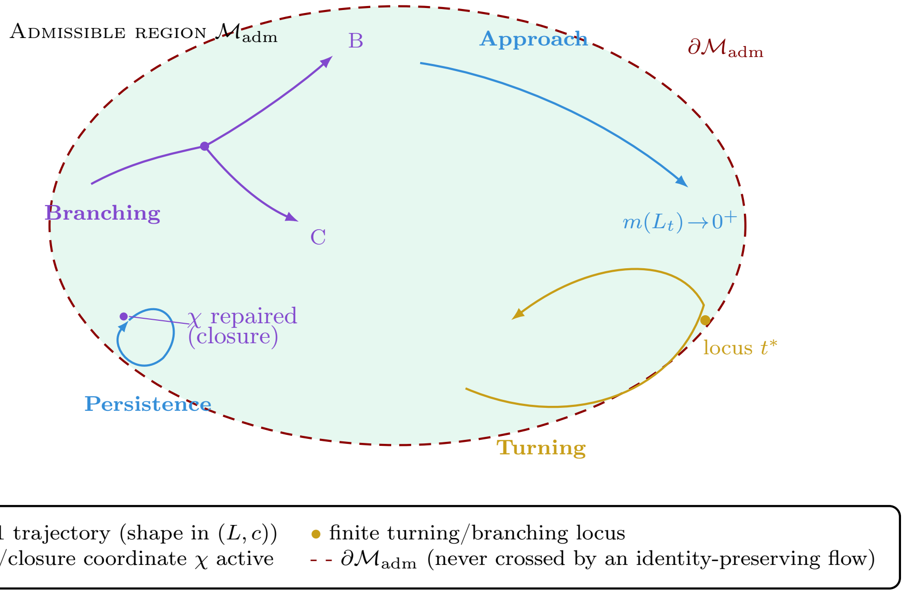

Figure 3: The structural motion landscape. A schematic, not to any corpus's actual scale: the admissible region $\mathcal{M}_{\text{adm}}$ (shaded) and its boundary $\partial\mathcal{M}_{\text{adm}}$, with the four Tier-1 trajectory-shape classes drawn as paths through it (persistence, approach, turning, branching) and one Tier-2 relational annotation (a route/closure coordinate χ being repaired on an otherwise persistent trajectory) shown as it would attach to a Tier-1 shape. Recoverable motion, recurrence, and commutation are relations that do not reduce to a single path through this landscape and are not depicted here; they are treated separately in Figures 4 and 5. This figure fixes the visual grammar (basin shading, boundary style, trajectory color by tier, locus markers) reused in every subsequent figure.

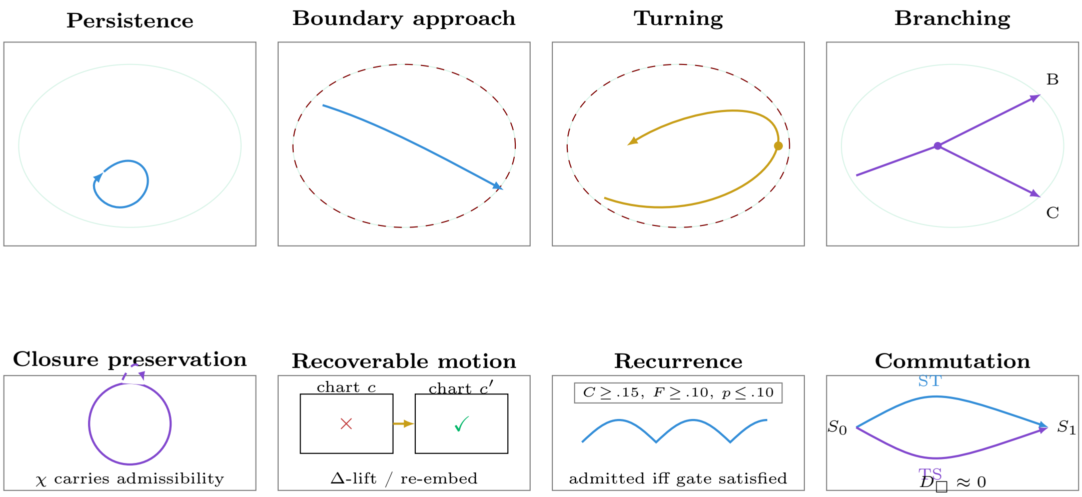

Figure 4: The eight structural motion classes. Top row: Tier-1 trajectory-shape classes, drawn in the visual grammar of Figure 3 (shaded admissible region, dashed boundary where relevant, gold locus marker, purple for an active route/closure coordinate). Bottom row: Tier-2 relational classes, each drawn as a relation rather than a single path — a coordinate attribution (closure preservation), a between-chart comparison (recoverable motion), a trajectory-versus-grammar test (recurrence), and a between-order comparison (commutation). No cross-domain numerical scale is implied by icon size or position; this is a classification diagram, not a measurement plot.

and 69% of boundary-adjacent (Giant) excursions clustering in 2011–2012 [10, 4]. The system approaches the low-margin frontier, crosses a physical boundary, and recovers to a higher-κ_{conn} state without triggering persistent Hard fragmentation [10]. The Margin-Confinement Law's later reinterpretation of FCC (Section 3) reframes this not as precarious near-miss survival but as admissibility-protected near-boundary compression: structurally inevitable under identity-preserving evolution, not a coincidence of the corpus tested.

6.2 Turning motion: the cosmological bounce

Admissible Boundary Routing [8] is the corpus's clearest instance of turning motion, and its effective-dynamics bounce mechanism is not a UNNS-internal invention: it is the standard loop quantum cosmology (LQC) bounce, established analytically and numerically in a well-known sequence of results [35, 36, 37] and reviewed since [38, 39], with the specific effective Friedmann-equation correction term $H^2 \propto \rho(1 - \rho/\rho_c)$ used to produce the bounce traceable to a specific derivation [40]; bounce cosmologies more broadly are surveyed in [41]. Three matched trajectories — classical Friedmann contraction (Dataset A), an effective LQC bounce (Dataset B), and Planck-2018-anchored ΛCDM expansion (Dataset C) — are compared through an orientation-sensitive route coordinate $s \in [-1, +1]$. Route A moves $-1 \to 0$ (terminal approach); Route C moves $0 \to +1$ (boundary recession); Route B moves $-1 \to 0 \to +1$: contraction, a finite turning locus at $H = 0,\ \rho = \rho_c$ (minimum scale factor $a_{\text{min}} = 2.468 \times 10^{-32}$), and expansion, with $\dot{a}$ reversing sign and the post-turning phase-sign vector approximately the negative of the pre-turning vector [8]. What is specific to this UNNS branch is not the bounce mechanism itself but the structural reading of it: treating the bounce as an instance of a general *turning* motion class, comparable in kind (though not in physical mechanism) to branching and approach elsewhere in the corpus.

Observed Pattern 6.1 (Turning-locus shielding). [Observed] Of 84,000 α-deformation rows tested along Dataset B's path, instability is not uniformly distributed: it concentrates in "near-bounce shell" regions on either side of the turning locus (491 unstable rows on each side) while zero unstable rows occur in the outer contraction/expansion regions *and zero occur at the exact bounce crossing itself*, yielding 98.83% α-admissibility persistence overall [8].

The source manuscript names this pattern **Hypothesis 9.1 (Turning-Locus Shielding)** and is explicit that it is a hypothesis, not a proven law: it has "not yet been causally explained," is scoped to one pilot dataset and one effective-LQC construction, and is stated as pending replication across other bounce models and grid refinements [8]. The present synthesis inherits that qualification: instability being localized *around* rather than *at* a turning locus is an observed pattern in this corpus, not yet a general property of turning motion. What is established more firmly is the role of orientation: under sorted-magnitude (unsigned) encoding, Datasets A and C become *structurally identical* (identical κ_{conn}, GR, A_κ, and α-vectors), formally proven magnitude-degenerate but route-distinct [8].

Framework Interpretation 6.2. A representation can preserve scale geometry while erasing route topology. Magnitude-only encodings erase the distinction between terminal approach and boundary recession, which is recovered only by signed orientation encoding [8]. This is the sharpest available illustration in the corpus that boundary coordinates and route topology are not the same thing (motion classes 5.2 and 5.3 are observationally conflatable under the wrong chart).

6.3 Branching motion: catastrophic stellar transition

Stellar Boundary Dynamics [9] evaluates a three-layer core-collapse supernova corpus — pre-supernova radial profiles (Phase A, 2 objects), post-collapse light curves (Phase B, 6 objects), and post-collapse spectral evolution (Phase C, 2 objects) — through 10 STRUC-PERC-I runs, all of which return FULL_PERCOLATION with zero Hard, Giant, or Tail outcomes [9]. The tri-domain ABC bridge geometry, however, resolves a global classification of **"A_to_B_contact_with_C_branching"**: weak A–B separation ($d_{AB} = 0.401$) contrasts with strong B–C and A–C separation ($d_{BC} = 1.287$, $d_{AC} = 1.365$) [9]. This motivates the branch's central structural proposition:

Proposition 6.3 (Internal Admissibility Is Not Cross-Regime Equivalence, after [9])**.** $\mathrm{Full}(A) \wedge \mathrm{Full}(B) \wedge \mathrm{Full}(C) \not\Rightarrow A \approx_{\text{bridge}} B \approx_{\text{bridge}} C$. *In the Stellar Boundary Dynamics corpus, internal Full-percolation in each of Phases A, B, and C does not imply structural equivalence of those phases under bridge geometry.*

Observed Pattern 6.4. [OBSERVED] Local admissibility survival is not, by itself, evidence that the pre- and post-catastrophe regimes occupy the same structural position. A system can branch — routing into more than one distinct downstream admissible regime — without any of the resulting regimes becoming inadmissible [9]. This is proposed by the source manuscript as a general principle (Conjecture 6.6, "Boundary Routing Conjecture": a catastrophic transition need not destroy admissibility; it may route among admissible regimes) but is explicitly scoped as a pilot-corpus finding, not a proven theorem [9].

7 Route Preservation and Closure

Three branches ask a structurally identical question in three physically unrelated settings: does a scalar-conserved quantity fully determine admissibility, or does admissibility additionally require preservation (or repair) of an underlying route/closure structure?

7.1 Charge

The Charge Boundary-Route Preservation Law [5], distilled from the six-phase Charge Boundary Routing I program [6], states the principle directly:

Principle 7.1 (after [5])**.** *For a charge-bearing transition T to be structurally admissible, $T \in \mathcal{M}_{\text{adm}} \Rightarrow (Q_i = Q_f) \wedge \mathrm{RouteCoherent}(T)$, but $(Q_i = Q_f) \not\Rightarrow T \in \mathcal{M}_{\text{adm}}$. Scalar charge balance is necessary but not sufficient.*

A positron, proton, positive pion, positive kaon, and W^+ boson all project to $Q/e = +1$ while occupying external-lepton, composite-baryon, composite-meson, strange-meson, and gauge-sector closures respectively [5, 6]. A same-charge control over $\binom{5}{2} = 10$ pairs, with $\Delta Q = 0$ for every pair by construction, finds `structural_route_pair_code` reaching GEOMETRIC PERSISTENCE/STABLE STRUCTURE with $\langle A_\kappa \rangle = 1.000$ while the trivial same-charge control encoding remains STRUCTURAL BOUNDARY/TRANSITIONAL STRUCTURE [6] — charge equality is fixed by design, yet a persistent structural signal remains. In the decisive Phase 3C contrast (48 mixed allowed, charge-violating, free-fractional, and route-incoherent candidates), the corpus remains globally connected under STRUC-PERC-I (42/42 completed ladders reach FULL_PERCOLATION), but under STRUC-I the `route_transition_code` encoding falls from BOUNDARY-STABILIZED ($\langle A_\kappa \rangle = 0.985$ in the Phase 3B allowed-only corpus) to STRUCTURAL BOUNDARY/TRANSITIONAL STRUCTURE ($\langle A_\kappa \rangle = 0.859$), while `closure_transition_code` remains stable at GEOMETRIC PERSISTENCE/BOUNDARY-STABILIZED ($\langle A_\kappa \rangle = 0.998$) [6]. Forbiddenness, in this corpus, is not graph disconnection; it is selective loss of route-transition admissibility.

7.2 Color confinement

QCD confinement is itself an established, decades-old subject of study — Wilson's original lattice formulation [57] and Greensite's survey of the confinement problem [58] both remain standard references — and Color Confinement as Admissibility-by-Closure [7] does not attempt to re-derive it. Instead it treats confinement as a structural, not dynamical, benchmark for the closure-preservation principle of this section: an internally real colored coordinate is not an admissible external output; attempted route extension toward isolation produces localized route tension; that tension resolves at a repair-threshold window into an admissible color-neutral composite route [7]. Over a 17-row repair-window ladder built from a derived boundary-pressure proxy $\Pi_{\text{boundary}}(r)$, the maximum value (0.766) occurs at $r = 1.221$ fm, immediately adjacent to the static-source level-crossing radius $r_c = 1.224 \pm 0.015$ fm reported by the underlying lattice data [59, 7], with a quark-mass-dependence extension and an independent flux-tube-structure study of the same static-source picture available in more recent lattice work [60, 61]. The source manuscript is explicit that this is a **conceptual manuscript with bounded diagnostic support**: the static spectrum is reconstructed from published Hamiltonian parameters rather than raw lattice output, Π_{boundary} is not a fitted physical potential, and the manuscript does not derive QCD confinement or the mass gap [7].

7.3 H-mode plasma

The H-mode itself is the original, empirically established edge transition this branch treats structurally: first reported at ASDEX [51] and since reviewed extensively, including threshold-scaling work directly relevant to the corpus used here [52, 53, 54]. Boundary-Route Preservation in H-Mode Plasma [12] extends the same structural language to tokamak edge physics via an event-level margin $m_{\text{edge,event}} = C_{\text{edge}} - F_{\text{route}}$, where F_{route} aggregates power-balance, transport, and timing fragmentation pressures and C_{edge} aggregates edge-response, density-support, geometry, and species-position scores [12]. Across the 92-event TCV corpus, the three margin corridors (negative leakage, boundary-ambiguous, positive boundary) are strictly ordered (Kruskal–Wallis $H = 53.85$, $p \ll 0.001$) and separate H-mode from L-mode occurrence at AUC$= 0.690$ [12]. In the independent TokaMark/MAST validation set, all five recovered h_mode_stable windows show a positive within-shot H-minus-L margin delta (minimum +1.062), confirming the ordering l_mode < lh_transition < h_mode_stable out-of-sample [12]. The source manuscript is explicit that standard plasma variables remain superior for binary L/H classification (LOO AUC = 1.000 versus 0.655 for the UNNS margin alone) and that the UNNS margin is a supportive structural diagnostic, not a replacement discriminator [12].

Framework Interpretation 7.2. Charge, color confinement, and H-mode plasma should not be read as sharing microscopic physics. Structurally, all three ask whether a physically realized transition maintains or restores a permitted route, and all three find that a scalar or binary summary (charge value, confinement label, L/H classification) is necessary but not sufficient to characterize admissibility: route/closure coordinates carry additional structural information in every tested corpus.

8 Representation and Recoverable Continuity

A recurring finding across the corpus is that an apparent structural failure is frequently a property of the representational chart rather than of the underlying physical system, and that a locality-preserving transform can recover admissibility without altering the physical system itself.

8.1 Neutrino Δ-lifting: the clearest recovery result

Across the 67-ladder neutrino detector corpus (shared by [4] and [3]), all nine raw-fragmented ladders (three Hard, six Tail) recover to FULL_PERCOLATION under Δ-lifting, with GR = 1.000 and zero isolated nodes in every recovered case — a 100% (9/9) recovery rate [4, 3]. FCC-like states (tail dominance ≥ 0.95) expand from 5 to 34 instances under the same transform (6.8×) [3]. This is not reported as unqualified: six new degradations also occur under Δ-lifting, and both source manuscripts trace all six to ladder-length contraction ("n-poverty"), not to genuine loss of admissibility — for example, `sig2pp`'s row count falls from 3,935 to 73 (1.9% retention) under the transform [3].

8.2 Extreme transitions: raw versus differenced observables

Beyond Fragmentation [10] reports the same pattern in two unrelated domains. A Type Ia supernova raw-magnitude ladder returns HARD_FRAGMENTATION (GR = 0.952, Theorem 3.1 active), while its Δ-magnitude and curvature representations both return FULL_PERCOLATION (GR = 1.000) [10]. A Nevada earthquake corpus shows the full spectrum from FULL_PERCOLATION at proximal stations to HARD_FRAGMENTATION at the most distant teleseismic station (IU.HRV, ∼3,100 km), a pattern the manuscript diagnoses as Representation-Induced Structural Collapse driven by propagation-distance attenuation [10]. Crucially, the manuscript also reports where the recovery mechanism *fails*: at IU.HRV, differencing alone does not eliminate the collapse, and the entire 29-event nuclear-explosion corpus shows no FULL_PERCOLATION verdicts at any station-event pair under any tested representation (see Section 12).

8.3 Admissible Cluster Geometry: chart transitions as transport operators

Admissible Cluster Geometry [3] formalizes three explicit **structural transport mechanisms** between basins: ε-corridor bridging, Δ-lifting as a chart transition, and deep-embedding as an admissibility lift. In the same corpus, 21 of 23 deep-learning-embedded neutrino ladders achieve GR = 1.000 with zero isolated nodes, including a full Hard-to-Full crossing under embedding change alone (`h_SigSB_significance_2`: HARD_FRAGMENTATION, GR = 0.985 under TMVA → FULL_PERCOLATION, GR = 1.000 under deep-learning embedding) [3].

8.4 Galaxies: representation sensitivity without full recovery collapse

Galaxy Structural Fingerprints [11] reports the corpus's most carefully qualified representation-sensitivity result. Under coverage-geometry transformations, retrieval degrades sharply and non-uniformly: leave-one-radius-out top-1 recovery falls to 0.551, and fixed-count radial coverage — the most aggressive tested transformation — falls to 0.050, while mass-to-light sensitivity remains comparatively mild at 0.517 [11]. The source manuscript's own reading is that "radial coverage and point count are more active coordinates in fingerprint expression than single-point deletion or reasonable mass-to-light variation" [11] — representation choice is not a uniform nuisance parameter; some representational axes are far more structurally consequential than others.

Framework Interpretation 8.1. Representation is not neutral preprocessing in this corpus: raw versus Δ-lifted neutrino ladders, raw versus normalized chemistry trajectories, coarse versus refined helium reconstruction, raw supernova observables versus Δ-magnitude/curvature, magnitude-only versus orientation-sensitive cosmological encoding, and galaxy radial-coverage geometry all change the structural verdict returned for the same underlying system [4, 3, 10, 2, 8, 11]. The corollary that follows is:

$$\text{physical process} \neq \text{observational chart} \neq \text{structural verdict.}$$

9 Recurrence and Transformation Algebra

Two further branches introduce motion classes that are not exhausted by monotonic boundary travel: recurrence through a temporal grammar, and approximate commutation between two transformation orders.

9.1 Recurrence: an integer-depth grammar and its domain boundary

"Time crystal" names an established line of physics this branch is structurally adjacent to but does not itself claim to instantiate: the original proposal and the no-go theorem that reshaped it [42, 43], the Floquet time-crystal formulation that survived that theorem [44, 45], its first experimental observations [46, 47], a subsequent review [48], and the quasiperiodically driven and quasicrystal-adjacent extensions most relevant to the multi-clock branch below [49, 50]. The UNNS branches synthesized here do not test whether any physical system is a time crystal in that literature's sense; they test whether a specific structural admission grammar, built independently of that physics literature, recognizes a candidate signal as temporally recurrent, and the "domain boundary" language of Finding 9.1 below refers to the grammar's scope, not to a claim about the referenced physics. Manuscript I of the time-crystal sequence [13] freezes a recurrence-depth structural metric $C(q)$, a recurrence-family contrast F, and a shuffle-null significance test p, with a joint admission gate $C(q_0) \geq 0.15$, $F \geq 0.10$, $p \leq 0.10$ frozen against a ten-record known-physics calibration corpus before any prospective test. Two prospective candidates are correctly admitted: C001 ($q_0 = 4$, $C = 0.5483$, $F = 0.3617$, $p = 0.0149$, temporal recurrence, versus a no-recompilation control returning no temporal order) and C002 ($q_0 = 2$, $C = 0.5191$, $F = 0.5064$, $p = 0.0050$, versus a matched $\varepsilon{=}0$ control that returns no temporal order *despite a higher raw* $C = 0.6250$ — the frozen gate is explicitly not a raw-magnitude threshold) [13]. A third candidate, C003, a robust experimental two-clock discrete time quasi-crystal (DTQC), fails the same frozen gate both blind and on a matched control ($q_0 = 6$, $C = 0.1988$, $F = 0.0934$, $p = 0.9602$) [13].

The source manuscript is careful about what this means:

> *"We do not claim 'the DTQC has no temporal order.' The correct, bounded statement is: under the frozen dual-clock adapter and the integer-depth recurrence grammar, the tested robust DTQC regime did not enter the supported temporal-recurrence class... It does not mean absence of physical temporal order... only that this frozen adapter and grammar did not supply one." [13]*

This is a **recurrence-grammar domain boundary**, not a falsification of temporal order in the candidate.

A companion manuscript, Beyond Integer Depth [14], develops — on a separate, independently frozen development corpus (Huang, Luo, and, after a locked transfer test, Zhu) that deliberately excludes C003 throughout — a multi-clock grammar (`MC_GRAMMAR_v001`) built around four candidate representations, of which one, fractional-cover decomposition ($M_{\text{frac}} = R^2_{\text{full}}(d^*) - R^2_{\text{axis}}(d^*)$), is retained as the primary decision coordinate after achieving AUC= 1.000 against all four development control families [14]. When this independently frozen grammar is finally applied to C003, it does not admit the candidate either, but through a qualitatively different failure mode: C003's source-anchor coordinate P_{src} fails at the worst possible value ($p = 1.000$, "source unanchored") while its fractional-cover coordinates ($J_{\text{frac}} = +0.911$, $M_{\text{frac}} = +0.596$) are simultaneously the strongest seen anywhere in the study [14]. The manuscript's own diagnosis is structural: the grammar implicitly assumes a parent-anchored-then-fractional hierarchy, and C003 exhibits weak parent-anchoring together with strong fractional organization — a **second, independent domain boundary**, distinct from the first, inside multi-clock temporal organization itself [14].

Observed Pattern 9.1. [OBSERVED] Two independently developed and independently frozen UNNS temporal recurrence grammars, tested on non-overlapping development corpora, both fail to admit the same candidate (C003), via two structurally distinct failure mechanisms. Neither manuscript treats this as evidence against temporal order in the candidate; both treat it as evidence that their respective grammar's domain of application is narrower than initially scoped [13, 14].

9.2 Commutation: scale and time in forced isotropic turbulence

Reproducible Scale–Time Commutation Structure [15] asks whether constructing a structural object's routing ancestry by coarsening scale and then advancing time ("ST") substantially agrees with advancing time and then coarsening scale ("TS"), quantified by a stitching defect $D_\square = \mathrm{JSD}(\mathrm{ST}, \mathrm{TS})/\ln 2 \in [0, 1]$. Under a preregistered two-pilot design on disjoint 256^3 Johns Hopkins Turbulence Database cutouts (zero shared grid points, zero shared stored frames), six of eight frozen criteria (R1, R2, R4, R5, R6, R8) replicate in the independent Pilot B sample, including the principal commutation-survival criterion at $z = 36.0$, $p = 0.0099$ [15]. The manuscript's own summary of what did and did not replicate is exact and should not be compressed further:

> *"The route mechanism reproduces; the scalar admissibility strength of the same ladder and the physical-intensity localization of its extreme tail do not." [15]*

Where non-commutation does occur, it is not diffuse: more than 90% of the 3,962 eligible objects in Pilot B lie at exactly $D_\square = 0$, and the elevated-$D_\square$ minority localizes specifically around scale- and time-branching events (both replicated at $p = 0.00020$), not around merging or aggregate restructuring (not replicated, $p = 1.0$) [15].

Observed Pattern 9.2. [OBSERVED] Scale-then-time and time-then-scale transformation orders approximately commute in the tested turbulence corpus; the sparse minority of cases where they do not commute is concentrated around branching structures specifically, not around merging or generic restructuring. This extends the taxonomy from properties of a single trajectory to a relation between two transformations applied to the same object.

10 Predictive Admissibility and Basin Occupancy

The persistence-geometry results of Section 4 rest on an explicit falsification protocol that deserves separate emphasis, since it is what licenses treating basin co-occupancy (Interpretation 4.1) as more than a curve-fitting coincidence. Canonical Structures in Admissibility Space [2] tests its five coherent physical domains (helium, cosmology, protein, and two neutrino sub-domains) against a 650-ladder adversarial corpus (uniform, Pareto, random-walk, and shuffle surrogates) under a hierarchical falsification criterion requiring near-zero adversarial penetration and positive within-domain self-similarity. Five domains pass cleanly (adversarial penetration $\rho = 0.000$ in four cases); four neutrino sub-domains (deep-learning, TMVA, raw-signal, raw-background) are explicitly *not* falsified but instead flagged as internally **bifurcated** (negative within-domain cosine similarity, as low as -0.182), meaning the standard penetration test is inapplicable to them until re-evaluated on the Δ-lifted canonical chart [2]. The uniform adversarial class shows zero penetration against every real domain tested ("cleanly separated everywhere"); Pareto and random-walk surrogates show weak penetration (0.109–0.126) specifically against the neutrino deep-learning sub-domain, and shuffle surrogates show weak penetration (0.045) against the TMVA sub-domain [2].

Observed Pattern 10.1. [OBSERVED] The program's validation protocols have moved beyond exploratory pattern-finding toward adversarial and preregistered falsification: hierarchical adversarial testing in the predictive-admissibility branch [2]; preserved negative falsification within Admissible Cluster Geometry's own explicit falsification-condition list [3]; a frozen, preregistered recurrence grammar with a cryptographic lock-before-reveal protocol in the time-crystal branches [13, 14]; and a preregistered, non-overlapping two-pilot replication design in turbulence [15]. UNNS structural claims increasingly have to survive controls that were not used to construct the metric being tested, rather than merely fitting the corpus that motivated them.

11 Cross-Domain Evidence Matrix

Table 3 summarizes, for each of the thirteen branches, the initial regime, transformation, dominant motion class(es), boundary behavior, representation effect, and validation type, drawing only on the quantitative results and verdicts documented in Sections 4–10.

Motion class	**Physical evolution**	**Chart transformation**	**Analytical operator**	**Temporal evolution**
Persistence	Voyager 1 sustaining Full percolation across most of 2011–2017 outside the crossing epoch [10, 4]	*no corpus instance identified (galaxy fingerprint retrieval under unchanged preparation [11] is an identity baseline, not a chart change, and is not counted here)*	Zero regime flips across 7 κ-grid configurations (1,316 evaluations) [3]; the 9×9 deformation-field sweep in fundamental-constant space [2]	*no corpus instance identified*
Boundary approach	Voyager 1's physical approach to the heliopause, $m(L_t) \to 0^+$ [10, 4]	Magnitude-only encoding collapsing the approach/recession distinction between Routes A and C [8]*	*no corpus instance identified*	*no corpus instance identified*
Turning	LQC bounce, Dataset B: contraction → finite turning locus → expansion [8]	Magnitude-only encoding rendering Routes A and C structurally identical, erasing orientation (Interpretation 6.2) [8]*	*no corpus instance identified*	*no corpus instance identified*
Branching	Core-collapse routing into distinct Phase B/C downstream regimes [9]	*no corpus instance identified*	*no corpus instance identified*	*no corpus instance identified*
Closure preservation	Charge-conserving particle transitions [5, 6]; H-mode edge transition [12]	*no corpus instance identified*	H-mode diagnostic-confidence correction separating signal from missing-data artifact in the route-preservation verdict [12]	*no corpus instance identified*
Recoverable motion	*no corpus instance identified (Voyager's physical κ_{conn} rebound,* 1.6–2.4× *after the 2012 crossing [10], is boundary-approach/persistence behavior under one fixed chart, not chart-mediated recovery; see Section 8)*	Δ-lifted recovery of 9/9 fragmented neutrino ladders [4, 3]; SN Ia raw-magnitude to Δ-magnitude recovery [10]	Deep-embedding recovery: 21/23 neutrino ladders reach GR = 1.000, including a full Hard-to-Full crossing under embedding change alone [3]	*no corpus instance identified*
Recurrence	*no corpus instance identified*	*no corpus instance identified*	Frozen admission gate $C(q_0) \geq 0.15$, $F \geq 0.10$, $p \leq 0.10$ applied to C001/C002 [13]; candidate C003 evaluated under two independently constructed grammars (integer-depth vs. multi-clock) [13, 14]	The time-ordered recurrence-depth sequence $C(q)$ traced along candidates C001/C002, prior to gate application [13]
Commutation	*Does not occupy a single cell; see discussion below.*			

Table 2: Motion class × transformation type, with concrete corpus instances. A blank cell is a genuine absence, not an oversight: no represented branch has yet tested that combination. Entries answer one of two distinct questions, which the accompanying text distinguishes: most entries report a transformation that *instantiates* the motion class, but an entry marked with an asterisk (*) instead reports a transformation that *alters the observability* of the motion class — for example, a magnitude-only chart that erases the orientation needed to tell approach from turning [8] — without itself producing the underlying motion.

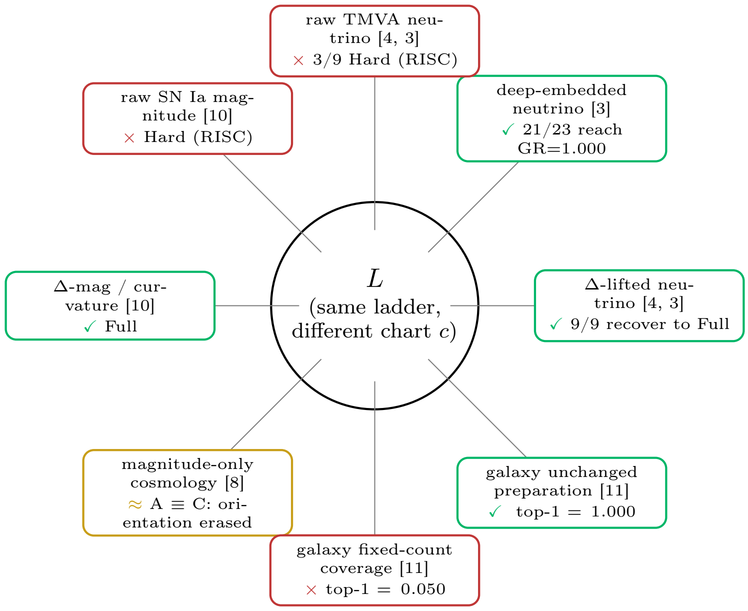

Figure 5: Representation can hide or recover structure. Eight charts c applied to physically unrelated ladders L (neutrino, supernova, cosmological, galactic), each pair drawn from the same underlying physical system so that only the chart differs. Green boxes (✓) reach an admissible or recovered verdict; red boxes (×) reach Hard or severely degraded verdicts on the same or a paired system; the gold box (≈) marks a chart that does not fail but instead erases a distinction (terminal approach versus boundary recession) that a different chart preserves. No single chart is uniformly correct or uniformly representation-neutral across this set; the specific numbers are drawn from Section 8 and are not implied to be commensurable with each other across domains.

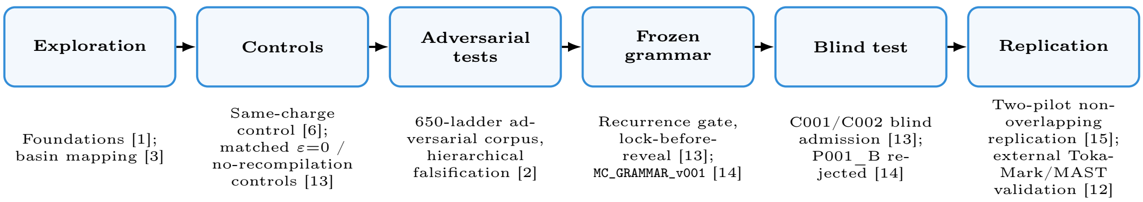

Figure 6: Validation architecture. The program's methodological maturation, read across branches rather than within any one of them: later work increasingly tests earlier metrics against controls, adversarial surrogates, frozen (pre-registered) admission criteria, genuinely blind prospective candidates, and independent out-of-sample replication, rather than validating a metric only against the corpus that motivated it. Not every branch passes through every stage, and the ordering is a methodological progression across the program's history, not a pipeline every individual finding is claimed to have completed; Section 12 records where a stage-appropriate test (a blind prospective candidate, an independent replication sample) did not confirm the tested hypothesis.

Table 3: Cross-domain evidence matrix. Motion classes refer to Section 5: Pe = persistence, Ap = approach, Tu = turning, Br = branching, Cl = closure preservation, Rc = recoverable motion, Re = recurrence, Co = commutation.

Branch	**Initial regime**	**Transformation**	**Class**	**Boundary behavior**	**Representation effect**	**Validation type**
Predictive admissibility [2]	Admissible, domain-scattered	Deformation-field sweep (9×9 grid)	Pe	No hard violations; basin co-occupancy across ≥ 14 domains	4 neutrino sub-domains bifurcated, not falsified	650-ladder adversarial corpus, hierarchical falsification
Boundary-mediated continuity [3]	Admissible, internally stratified	Grid-resolution and chart-transport sweep	Pe, Rc	Localized stitching defects (80.4% of glass HF cases: 1 isolated node)	Δ-lift: 9/9 neutrino recovery; 0/1316 grid-invariance flips	7-configuration grid invariance; two-stage before/after transform
Non-crossability [4]	Admissible	Identity-preserving flow	Ap, Rc	$m(L_t) \to 0^+$ without crossing; $p < 3 \times 10^{-4}$ genuine-crossing bound	RISC across Voyager, seismic, neutrino, SN Ia channels	Source-reported N_{tot} = 15,401 evaluations (aggregate accounting unresolved in this synthesis, Sec. 2), spanning 14 physical + 1 biological + 1 astrophysical + 1 detector domain
Charge boundary routing [5, 6]	Charge-bearing object/transition	Static classification; 38 allowed transitions; 48 mixed boundary tests	Cl	Route-transition admissibility collapses (0.985→0.859) while connectivity persists (42/42 FP)	Route/closure encodings percolate where charge-value encodings fragment	Same-charge control (10 pairs, ΔQ=0); allowed/forbidden contrast corpus
Color confinement [7]	Internal colored coordinate	Route extension toward isolation	Cl	Repair-threshold window at $r \approx 1.22$ fm, adjacent to $r_c = 1.224$ fm	4/8 raw local descriptors HF; boundary-pressure proxy reaches FP/Stable	Lattice-QCD-derived diagnostic corpus (Bulava, Baker); bounded diagnostic status
Cosmological routing [8]	Admissible	Contraction / bounce / expansion (3 matched routes)	Tu	Finite turning locus; 98.83% α-admissibility persistence; shielding is a stated hypothesis	Magnitude-only encoding erases A/C orientation distinction (proven degenerate)	84,000-row α-deformation sweep; A–B–C orientation-sensitive bridge
Stellar boundary dynamics [9]	Admissible (pre-supernova)	Catastrophic core collapse	Br	10/10 FP; internal admissibility $\not\Rightarrow$ cross-regime bridge equivalence	Terminal-snapshot and spectral-proxy representations, not time-resolved	Tri-domain ABC bridge geometry; object-matched coherence test
Extreme transitions [10]	Admissible, near-boundary	Explosive / impulsive / seismic / nuclear forcing	Ap, Rc	FCC (TD>0.80, GR≥0.97); Voyager recovers post-crossing	Raw SN Ia magnitude HF → Δ-mag/curvature FP; NK corpus never reaches FP	Cross-domain replication (astrophysical, seismic, nuclear, collision, heliospheric)

continued on next page

Table 3 continued

Branch	**Initial regime**	**Transformation**	**Class**	**Boundary behavior**	**Representation effect**	**Validation type**
Galaxy structure [11]	Admissible / stratified basin	Perturbation sweep; radial-coverage change	Pe	110/121 Stable Structure vs. 11 Weak Persistence; only 17/121 reach FP (adaptive κ_{conn} only)	Fixed-count coverage collapses top-1 retrieval to 0.050	Held-out galaxy-balanced transfer test (5-fold); Gate B/C retrieval tests
H-mode plasma [12]	Fragmentation-dominated leakage	Edge transition to improved confinement	Cl	Strict corridor ordering (Kruskal–Wallis $p \ll 0.001$); 5/5 external windows confirm	Diagnostic-confidence correction distinguishes signal from missing-data artifact	9-shot pilot + 92-event TCV corpus + 5-window external TokaMark/MAST validation
Time crystal [13]	Candidate temporal recurrence	Frozen recurrence-depth grammar	Re	2/2 prospective DTC candidates admitted; DTQC candidate encounters domain boundary	Grammar explicitly representation-bound, not a claim about physical absence	10-record frozen calibration; blind prospective test; cryptographic lock-before-reveal
Multi-clock recurrence [14]	Candidate multi-clock organization	Independently frozen multi-clock grammar	Re	Prospective positive test rejected (P001); same DTQC candidate fails a second, distinct grammar	Parent-anchored vs. fractional-primary organization not jointly representable by v001	Firewalled development corpus (Huang, Luo, Zhu); genuinely blind external prospective test
Turbulence (JHTDB) [15]	Routed velocity-field objects	Scale transform vs. time transform, both orders	Co	Sparse non-commutation (<10% of objects), localized at branching events	R3 (scalar admissibility) and R7 (intensity localization) fail to replicate	Preregistered, non-overlapping two-pilot replication (8 frozen criteria)

12 Negative Results and Limits

Consistent with the source program's practice, this synthesis treats negative and boundary-encountering results as load-bearing rather than as an appendix. The emerging structure was not obtained by retaining every positive result and discarding failures; several proposed generalizations failed in specific, documented ways, and those failures are part of what defines the domain of each motion class.

- **Turbulence: partial, not full, replication.** Of eight preregistered criteria, R3 (scalar admissibility strength reaching GEOMETRIC PERSISTENCE) and R7 (physical-intensity localization of the extreme stitching-defect tail) fail to replicate in the independent Pilot B sample; R3 in particular is described by the source manuscript as "a genuine, unexplained divergence," 0.078 below threshold and well outside the precision-rerun band [15]. The formal classification is *Structural Partial Replication*, not Core Replication.
- **Two grammars, one unadmitted candidate.** Both the integer-depth time-crystal grammar [13] and the independently developed multi-clock grammar [14] fail to admit the same quasi-periodic candidate (C003), via two different mechanisms (Finding 9.1). The multi-clock grammar additionally fails its own genuinely blind prospective positive test (candidate P001_B), which the source manuscript states plainly: "PROSPECTIVE FAILURE — CANDIDATE REJECTED" [14].
- **Galaxy transfer does not clear its confirmation gate.** Every held-out model that adds static whole-galaxy chamber descriptors to a local radial baseline performs *worse* than the baseline alone (best static model RMSE 0.18428 versus baseline 0.18562; the full-signature model 0.19455, a -3.27% degradation) [11]. The one channel showing a positive transfer signal, the full $\rho(\kappa)$ curve, improves prediction in 4 of 5 folds but is explicitly reported as not clearing the manuscript's full registered confirmation gate [11]. The source manuscript's own framing is that this is informative about *architecture* (static whole-galaxy descriptors are the wrong predictive unit), not a falsification of the fingerprint's existence [11].
- **Recovery is not universal.** Δ-lifting recovers 9/9 fragmented raw neutrino ladders but also introduces six new degradations, traced to extreme ladder-length contraction under the same transform [3, 4]. In Beyond Fragmentation, differencing fails to recover the most severely propagation-distorted seismic station (IU.HRV) and never produces a single FULL_PERCOLATION verdict anywhere in the 29-event nuclear-explosion corpus under any tested representation [10].
- **Turning-locus shielding is a hypothesis under test, not a theorem.** Section 6.2's Finding 6.1 is explicitly scoped by its source manuscript to one pilot dataset and one effective-LQC construction, with replication across other bounce models named as future work [8].
- **Stellar branching is a corpus-level pilot finding.** Proposition 6.3 is drawn from a 10-object pilot corpus; the source manuscript explicitly states that its structural claims are corpus-level findings, not universal theorems, and that its Boundary Routing Conjecture is a proposed general principle, not one derived from first principles [9].

Framework Interpretation 12.1. The negative results above are not evenly distributed across the taxonomy: they cluster specifically at the edges of each motion class's stated domain —

a grammar's representational boundary (recurrence), a transform's length-contraction failure mode (recoverable motion), a localization criterion's unexplained divergence in one physical regime (commutation), and a predictive architecture's mismatch with a static descriptor (persistence transfer). This is consistent with each motion class being a real, corpus-supported distinction with a specific and discoverable domain of validity, rather than a universal solvent.

13 Toward a Structural Motion Principle

The results of Sections 6–10 motivate a synthesis-level principle. Consistent with the claim-tier discipline of Section 1, it is stated here as a framework-level interpretation, not a theorem: no single branch corpus establishes it, and no cross-branch statistical test in this manuscript establishes it either.

Structural Motion Principle (proposed synthesis-level interpretation). *A physically realized system is characterized jointly by the admissible structural region it occupies and by the class of transformations through which it can move while preserving, changing, or recovering structural identity. The structural characterization of physical realizability is not exhausted by admissible* states*; it also requires admissible* trajectories *and admissibility-relevant* relations among transformations — *the distinction, respectively, between the Tier-1 and Tier-2 classes of Section 5.1.*

This principle organizes, without collapsing, the eight motion classes of Section 5: persistence and boundary approach describe how a trajectory can remain inside $\mathcal{M}_{\mathrm{adm}}$; turning and branching describe how it can reorganize at a boundary without leaving $\mathcal{M}_{\mathrm{adm}}$; closure preservation and recoverable motion describe how admissibility can survive, or be restored under, a change of representational chart; and recurrence and commutation extend the vocabulary from single trajectories to relations between temporal grammars and between transformation orders, respectively.

14 Open Problems

The following are stated as open problems, in the sense used throughout the source branches: questions the present corpus is consistent with but does not resolve.

O1. A common metric structure. Whether the eight motion classes admit a shared metric or coordinate system on $\mathcal{M}_{\mathrm{adm}}$ in which "distance to boundary," "turning locus," and "branching angle" are commensurable across domains, rather than domain-specific constructions as at present.

O2. Domain-independent invariants of motion class. Whether a system's motion class (as opposed to its instantaneous state) can be predicted from structural properties of its governing dynamics, prior to running the relevant UNNS instrument.

O3. Chart equivalence. Admissible Cluster Geometry's own open conjecture — whether the bridgeability relation $\sim_{\mathcal{K}}$ is a global equivalence relation on all of $\mathcal{M}_{\mathrm{adm}}$, not merely on the tested corpus [3] — bears directly on whether "recoverable motion" (motion class 5.6) is a general property or a corpus-scoped regularity.

O4. Route equivalence. Whether a single formal notion of "route" (as used in charge, color confinement, and H-mode plasma; Section 7) can be given a domain-independent definition, or whether "closure preservation" remains three structurally analogous but formally distinct constructions.

O5. A boundary metric for turning and branching. Whether the turning-locus shielding pattern of Finding 6.1 and the branching-index construction of Stellar Boundary Dynamics [9] are instances of one underlying boundary-curvature quantity.

O6. Predictive transition probabilities. Whether the program's motion-class taxonomy can be extended from classification (which class does this trajectory belong to?) to prediction (given a system's motion class in one domain, what is the probability distribution over its downstream regime?).

O7. Observational versus ontological invariance. Whether the representation-sensitivity results of Section 8 converge, as more domains are tested, toward a stable list of representational axes that are always structurally active (as galaxy radial coverage appears to be [11]) versus axes that are domain-specific nuisance parameters.

Conjecture 14.1. [Conjecture] There exists a domain-independent taxonomy of structural motion, of which the eight classes identified here are instances, applicable beyond the thirteen branches synthesized in this manuscript. This is explicitly not established by the present corpus and should not be read as more than a research direction motivated by it.

15 Conclusion

The cross-domain evidence assembled here does not suggest that cosmology, core-collapse supernovae, charge-bearing particle transitions, color confinement, tokamak plasma edges, galactic rotation curves, forced isotropic turbulence, and discrete time-crystalline recurrence share one microscopic dynamics. It suggests something narrower and, within the scope of the tested corpora, better supported: once represented structurally within the UNNS admissibility framework, these physically unrelated systems repeatedly exhibit a restricted vocabulary of motion. They persist within basins [11, 2]; they approach boundaries without necessarily crossing them [4, 10]; they turn at finite loci [8]; they branch into distinct admissible regimes [9]; they preserve or repair closure routes [5, 6, 7, 12]; they recover continuity under chart changes [4, 3, 10]; they recur under temporal grammars, and in doing so expose the boundaries of those grammars [13, 14]; and in at least one tested case they exhibit approximate commutation between two transformation orders, with the exceptions to that commutation themselves structurally localized [15].

The object of study that emerges from reading these thirteen branches together is therefore not merely admissible structure, but admissible *structural motion.* This does not reduce the UNNS Substrate to a theory of motion. Rather, it identifies structural motion as a distinct layer within a broader architecture concerned with how structures are generated, represented, admitted, organized, transformed, and ultimately selected or predicted (Section 1.3). The taxonomy proposed here (Section 5) is offered at the framework-interpretation tier: it organizes what the corpus currently shows, names the eight recurring classes precisely enough to be checked against new branches as they are developed, and is deliberately silent — via the negative results of Section 12 and the open problems of Section 14 — about how far beyond the tested domains that organization extends.

References

[1] UNNS Substrate Research Program. *Foundations of the UNNS Substrate: From Universal Admissibility to Structural Regime Theory — A Cross-Domain Synthesis of Persistence, Boundary Behavior, Operator-Selective Response, and the Geometry of Structural Admissibility.* Foundation Document, 2026.

[2] UNNS Substrate Research Program. *Canonical Structures in Admissibility Space: Persistence Geometry and Empirical Basin Occupancy Across Physical Systems.* Synthesis Manuscript v1.0, 2026. https://ukbbi.github.io/UNNS/projects/regime_synthesis/predictive_admissibility_search/CanonicalStructuresinAdmissibilitySpace.pdf. Public reference: "How Physical Systems Find Their Place in Admissibility Space," https://unns.tech/research/how-physical-systems-find-their-place-in-admissibility-space.

[3] UNNS Substrate Research Program. *Admissible Cluster Geometry: Recoverable Connectivity in Realizability Space.* Working Manuscript, 2026. https://ukbbi.github.io/UNNS/projects/regime_synthesis/boundary-mediated_structural_continuity/AdmissibleClusterGeometry.pdf; dashboard: https://ukbbi.github.io/UNNS/projects/regime_synthesis/boundary-mediated_structural_continuity/regime_map_analysis_v3.html. Public reference: "How Admissible Structures Form Connected Worlds," https://unns.tech/research/how-admissible-structures-form-connected-worlds.

[4] UNNS Substrate Research Program. *The Margin-Confinement Law: Structural Non-Crossability in Admissibility Space, Derived from the Universal Structural Law and the Percolative Realizability Principle.* Foundational Theory Manuscript, 2026. https://ukbbi.github.io/UNNS/projects/regime_synthesis/non-crossability/TheMargin-ConfinementLaw.pdf; neutrino corpus: https://ukbbi.github.io/UNNS/projects/regime_synthesis/non-crossability/neutrino_corpus_analysis.html. Public reference: "The Hidden Rule Behind Structural Survival," https://unns.tech/research/the-hidden-rule-behind-structural-survival.

[5] UNNS Substrate Research Program. *The Charge Boundary-Route Preservation Law: Value Conservation, Route Admissibility, and Structural Selection in Charge-Bearing Transitions.* Completed manuscript version, 2026. https://ukbbi.github.io/UNNS/projects/regime_synthesis/charge_boundary_routing/ChargeBoundary-RoutePreservationLaw.pdf.

[6] UNNS Substrate Research Program. *Charge Boundary Routing: Fractional Coordinates, Composite Closure, and Route-Preserving Transitions.* Working Manuscript, 2026. https://ukbbi.github.io/UNNS/projects/regime_synthesis/charge_boundary_routing/Charge_Boundary_Routing.pdf; dashboard: https://ukbbi.github.io/UNNS/projects/regime_synthesis/charge_boundary_routing/charge_boundary_routing_i_analytics.html. Public reference: "Electric Charge Has a Route," https://unns.tech/research/electric-charge-has-a-route.

[7] UNNS Substrate Research Program. *Color Confinement as Admissibility-by-Closure: A UNNS Boundary-Route Interpretation.* Conceptual manuscript with bounded diagnostic support, July 2026. https://ukbbi.github.io/UNNS/projects/regime_synthesis/color_confinement/ColorConfinementasAdmissibility-by-Closure.pdf; dashboard: https://ukbbi.github.io/UNNS/projects/regime_synthesis/color_confinement/color_confinement_analytics.html. Public reference: "The Physics of Forbidden Isolation: Color Confinement in the UNNS Substrate," https://unns.tech/research/the-physics-of-forbidden-isolation-color-confinement-in-the-unns-substrate.

[8] UNNS Substrate Research Program. *Admissible Boundary Routing: Structural Classification of Terminal Approach, Finite Bounce, and Cosmological Recession.* Working Manuscript, 2026. https://ukbbi.github.io/UNNS/projects/regime_synthesis/cosmological_boundary_routing/AdmissibleBoundaryRouting.pdf; dashboard: https://ukbbi.github.io/UNNS/projects/regime_synthesis/cosmological_boundary_routing/cosmological_boundary_

routing_analytics.html. Public reference: "When the Universe Reaches Zero but Does Not End," https://unns.tech/research/when-the-universe-reaches-zero-but-does-not-end.

[9] UNNS Substrate Research Program. *Stellar Boundary Dynamics: Catastrophic Transition as Routing Between Admissible Structural Regimes.* Pilot Manuscript, 2026. https://ukbbi.github.io/UNNS/projects/regime_synthesis/stellar_boundary_dynamics/StellarBoundaryDynamics.pdf; dashboard: https://ukbbi.github.io/UNNS/projects/regime_synthesis/stellar_boundary_dynamics/stellar_boundary_dynamics_analytics.html. Public reference: "How Catastrophe Routes Structure Instead of Destroying It," https://unns.tech/research/how-catastrophe-routes-structure-instead-of-destroying-it.

[10] UNNS Substrate Research Program. *Beyond Fragmentation: Admissibility and Coherent Collapse Across Extreme Physical Transitions.* Foundational theory and cross-domain empirical analysis, 2026. https://ukbbi.github.io/UNNS/projects/regime_synthesis/extreme_physical_transitions/BeyondFragmentation.pdf; dashboard: https://ukbbi.github.io/UNNS/projects/regime_synthesis/extreme_physical_transitions/unns_explosive_dynamics_analysis.html. Public reference: "The Edge of Collapse: How Coherence Survives Extreme Physical Forcing," https://unns.tech/research/the-edge-of-collapse-how-coherence-survives-extreme-physical-forcing.

[11] UNNS Structural Astrophysics Programme. *Galaxy Structural Fingerprints: A Multiscale Atlas of Persistence, Fragmentation, and Connectivity.* UNNS Substrate Research Collective, August 3, 2026. https://ukbbi.github.io/UNNS/projects/regime_synthesis/galaxy-structure_and_validation/Galaxy_Structural_Fingerprints.pdf; dashboard: https://ukbbi.github.io/UNNS/projects/regime_synthesis/galaxy-structure_and_validation/UNNS_Galaxy_Structural_Fingerprint_Analytics.html. Public reference: "The Structural Identity of Galaxies," https://unns.tech/research/the-structural-identity-of-galaxies. Underlying rotation-curve data: SPARC (Lelli, McGaugh & Schombert 2016).

[12] UNNS Substrate Research Program, UNNS-H Mode Project. *Boundary-Route Preservation in H-Mode Plasma: A UNNS Edge-Admissibility Analysis of TCV and TokaMark Data.* Working Manuscript, 2026. Dashboard: https://ukbbi.github.io/UNNS/projects/regime_synthesis/UNNS_plasma_H_Mode/unns_hmode_event_level_analysis.html. Public reference: "The Hidden Route Behind H-Mode Plasma Confinement," https://unns.tech/research/the-hidden-route-behind-h-mode-plasma-confinement. Data: TCV L-H threshold database (Zenodo 14996664); TokaMark/MAST public diagnostic arrays.

[13] UNNS Research Collective. *Prospective Structural Classification of Discrete Time-Crystalline Recurrence: Integer-Depth Closure, Blind Validation, and a Quasi-Periodic Domain Boundary.* UNNS Substrate Research Program, August 20, 2026. https://ukbbi.github.io/UNNS/projects/regime_synthesis/time_crystal/Prospective_Structural_Classification_of_Discrete_Time-Crystalline_Recurrence.pdf. Public reference: "Organized or Accidental? How a Frozen Grammar Reads Time-Crystalline Recurrence," https://unns.tech/research/organized-or-accidental-how-a-frozen-grammar-reads-time-crystalline-recurrence.

[14] UNNS Research Collective. *Beyond Integer Depth: Multi-Clock Recurrence, Prospective Falsification, and a Fractional-Primary Boundary — A Companion Study to the Integer-Depth Temporal-Recurrence Grammar.* UNNS Substrate Research Program, August 27, 2026. Archive location: https://ukbbi.github.io/UNNS/projects/regime_synthesis/UNNS_MULTI_CLOCK_RECURRENCE. Public reference: "The Time Crystal That Broke Two Grammars," https://unns.tech/research/the-time-crystal-that-broke-two-grammars.

[15] UNNS Substrate Research Program, Turbulence Branch. *Reproducible Scale–Time Commutation Structure in Forced Isotropic Turbulence* (JHTDB Pilot-B Replication). Frozen Replication Record, 2026. https://ukbbi.github.io/UNNS/projects/regime_synthesis/TURB_JHTDB/ReproducibleScale%E2%80%93TimeCommutationStructure.pdf; dashboard: https://ukbbi.

github.io/UNNS/projects/regime_synthesis/TURB_JHTDB/jhtdb_pilot_b_analytics.html. Archive: Zenodo DOI 10.5281/zenodo.22650769. Underlying data: Johns Hopkins Turbulence Database, isotropic1024coarse. Attribution: E. Perlman, R. Burns, Y. Li, C. Meneveau, "Data Exploration of Turbulence Simulations Using a Database Cluster," *Proceedings of the ACM/IEEE Conference on Supercomputing* (SC07), 2007.

[16] J. Guckenheimer and P. Holmes. *Nonlinear Oscillations, Dynamical Systems, and Bifurcations of Vector Fields*. Springer, 1983.

[17] S. H. Strogatz. *Nonlinear Dynamics and Chaos: With Applications to Physics, Biology, Chemistry, and Engineering*. Westview Press / Perseus Books, 1994 (2nd ed. 2015).

[18] Y. A. Kuznetsov. *Elements of Applied Bifurcation Theory*. Springer, 3rd ed., 2004.

[19] S. Wiggins. *Introduction to Applied Nonlinear Dynamical Systems and Chaos*. Springer, 2nd ed., 2003.

[20] A. Andronov and L. Pontryagin. "Systèmes grossiers." *Doklady Akademii Nauk SSSR* 14, 247–250, 1937. (Cited as reported in secondary sources, e.g. Guckenheimer & Holmes [16], §1.7.)

[21] M. M. Peixoto. "Structural stability on two-dimensional manifolds." *Topology* 1(2), 101–120, 1962.

[22] R. Thom. *Structural Stability and Morphogenesis: An Outline of a General Theory of Models*. Benjamin/Addison-Wesley, 1975.

[23] E. C. Zeeman. "Catastrophe theory." *Scientific American* 234(4), 65–83, 1976.

[24] M. Scheffer, S. Carpenter, J. A. Foley, C. Folke, and B. Walker. "Catastrophic shifts in ecosystems." *Nature* 413, 591–596, 2001.

[25] M. Scheffer, S. R. Carpenter, T. M. Lenton, J. Bascompte, W. Brock, V. Dakos, J. van de Koppel, I. A. van de Leemput, S. A. Levin, E. H. van Nes, M. Pascual, and J. Vandermeer. "Anticipating critical transitions." *Science* 338(6105), 344–348, 2012.

[26] J. Milnor. "On the concept of attractor." *Communications in Mathematical Physics* 99, 177–195, 1985.

[27] S. R. Broadbent and J. M. Hammersley. "Percolation processes I: Crystals and mazes." *Mathematical Proceedings of the Cambridge Philosophical Society* 53(3), 629–641, 1957.

[28] G. Grimmett. *Percolation*. Springer, 2nd ed., 1999.

[29] D. Stauffer and A. Aharony. *Introduction to Percolation Theory*. Taylor & Francis, rev. 2nd ed., 1994.

[30] G. Carlsson. "Topology and data." *Bulletin of the American Mathematical Society* 46(2), 255–308, 2009.

[31] H. Edelsbrunner and J. Harer. *Computational Topology: An Introduction*. American Mathematical Society, 2010.

[32] A. Zomorodian and G. Carlsson. "Computing persistent homology." *Discrete & Computational Geometry* 33(2), 249–274, 2005.

[33] H. E. Stanley. *Introduction to Phase Transitions and Critical Phenomena*. Oxford University Press, 1971.

[34] N. Goldenfeld. *Lectures on Phase Transitions and the Renormalization Group*. Addison-Wesley, 1992.

[35] A. Ashtekar, T. Pawlowski, and P. Singh. "Quantum nature of the big bang." *Physical Review Letters* 96, 141301, 2006.

[36] A. Ashtekar, T. Pawlowski, and P. Singh. "Quantum nature of the big bang: An analytical and numerical investigation." *Physical Review D* 73, 124038, 2006.

[37] A. Ashtekar, T. Pawlowski, and P. Singh. "Quantum nature of the big bang: Improved dynamics." *Physical Review D* 74, 084003, 2006.

[38] A. Ashtekar and P. Singh. "Loop quantum cosmology: A status report." *Classical and Quantum Gravity* 28, 213001, 2011.

[39] M. Bojowald. "Loop quantum cosmology." *Living Reviews in Relativity* 11, 4, 2008.

[40] V. Taveras. "Corrections to the Friedmann equations from loop quantum gravity for a universe with a free scalar field." *Physical Review D* 78, 064072, 2008.

[41] M. Novello and S. E. P. Bergliaffa. "Bouncing cosmologies." *Physics Reports* 463, 127–213, 2008.

[42] F. Wilczek. "Quantum time crystals." *Physical Review Letters* 109, 160401, 2012.

[43] P. Bruno. "Impossibility of spontaneously rotating time crystals: A no-go theorem." *Physical Review Letters* 111, 070402, 2013.

[44] D. V. Else, B. Bauer, and C. Nayak. "Floquet time crystals." *Physical Review Letters* 117, 090402, 2016.

[45] V. Khemani, A. Lazarides, R. Moessner, and S. L. Sondhi. "Phase structure of driven quantum systems." *Physical Review Letters* 116, 250401, 2016.

[46] J. Zhang, P. W. Hess, A. Kyprianidis, P. Becker, A. Lee, J. Smith, G. Pagano, I.-D. Potirniche, A. C. Potter, A. Vishwanath, N. Y. Yao, and C. Monroe. "Observation of a discrete time crystal." *Nature* 543, 217–220, 2017.

[47] S. Choi, J. Choi, R. Landig, G. Kucsko, H. Zhou, J. Isoya, F. Jelezko, S. Onoda, H. Sumiya, V. Khemani, C. von Keyserlingk, N. Y. Yao, E. Demler, and M. D. Lukin. "Observation of discrete time-crystalline order in a disordered dipolar many-body system." *Nature* 543, 221–225, 2017.

[48] K. Sacha and J. Zakrzewski. "Time crystals: A review." *Reports on Progress in Physics* 81, 016401, 2018.

[49] P. T. Dumitrescu, R. Vasseur, and A. C. Potter. "Logarithmically slow relaxation in quasiperiodically driven random spin chains." *Physical Review Letters* 120, 070602, 2018.

[50] S. Autti, V. B. Eltsov, and G. E. Volovik. "Observation of a time quasicrystal and its transition to a superfluid time crystal." *Physical Review Letters* 120, 215301, 2018.

[51] F. Wagner, G. Becker, K. Behringer, D. Campbell, A. Eberhagen, W. Engelhardt, G. Fussmann, O. Gehre, J. Gernhardt, G. v. Gierke, et al. "Regime of improved confinement and high beta in neutral-beam-heated divertor discharges of the ASDEX tokamak." *Physical Review Letters* 49, 1408, 1982.

[52] J. W. Connor and H. R. Wilson. "A review of theories of the L-H transition." *Plasma Physics and Controlled Fusion* 42, R1, 2000.

[53] Y. R. Martin, T. Takizuka, and the ITPA CDBM H-mode Threshold Database Working Group. "Power requirement for accessing the H-mode in ITER." *Journal of Physics: Conference Series* 123, 012033, 2008.

[54] F. Wagner. "A quarter-century of H-mode studies." *Plasma Physics and Controlled Fusion* 49, B1, 2007.

[55] F. Lelli, S. S. McGaugh, and J. M. Schombert. "SPARC: Mass models for 175 disk galaxies with Spitzer photometry and accurate rotation curves." *The Astronomical Journal* 152, 157, 2016.

[56] S. S. McGaugh, F. Lelli, and J. M. Schombert. "Radial acceleration relation in rotationally supported galaxies." *Physical Review Letters* 117, 201101, 2016.

[57] K. G. Wilson. "Confinement of quarks." *Physical Review D* 10, 2445, 1974.

[58] J. Greensite. *An Introduction to the Confinement Problem*. Lecture Notes in Physics, Springer, 2011 (2nd ed. 2020).

[59] J. Bulava, B. Hörz, F. Knechtli, G. Moir, C. Morningstar, M. Peardon, and S. Skinner. "String breaking by light and strange quarks in QCD." *Physics Letters B* 793, 493–498, 2019.

[60] J. Bulava, B. Hörz, and colleagues. "The quark-mass dependence of the potential energy between static quarks in full QCD." *Physics Letters B* 854, 138754, 2024.

[61] M. Baker, P. Cea, L. Cosmai, F. Cuteri, and A. Papa. "Unveiling the flux tube structure in full QCD." *European Physical Journal C* 84, 2024. DOI: 10.1140/epjc/s10052-024-13725-2.